10.

# Isolation and Biological Characterization of An Infectious Molecular Clone of HIV-1 CRF08_BC from China

**S. Kusagawa, R. Yang and Y. Takebe**

*Laboratory of Molecular Virology and Epidemiology, AIDS Research Center, National Institute of Infectious Diseases, Tokyo, Japan*

## Summary

We isolated the first HIV-1 infectious molecular clone (IMC) (designated as 00CN-HH040.NX22) for CRF08_BC that is responsible for IDU epidemic in southeastern China. 00CN-HH040.NX22 replicated to high titers in PBMCs and utilized only CCR5 as a coreceptor for entry. 00CN-HH040.NX22 showed the identical recombinant structure with CRF08_BC reference strain. A potential sequence signature unique to CRF08_BC was observed in the enhancer region of LTR. 00CN-HH040.NX22 will be a useful tool to delineate the biological and virological properties of CRF08_BC and may also be used in design for vaccine candidates to limit the epidemic in southeastern China.

## Introduction

The infectious molecular clones (IMCs) of HIV-1 have been critical tools for systemic evaluation for delineating the mechanisms of viral replication and pathogenesis.

Phylogenetic analyses of globally circulating viral strains have identified three distinct groups of HIV-1 (M, N, and O), and 11 genetic subtypes and subsubtypes (A, A2, B, C, D, F1, F2, G, H, J, and K), and 15 circulating recombinant forms (CRFs) within the major group (M). Two closely-related CRFs, CRF07_BC and CRF08_BC, are emerging strains that play a critical role in the epidemic among injecting drug users (IDUs) in China [1, 2], where the cumulative number of HIV cases would be expected to reach 10 million by 2010 with the current

rate of increase (30%) [3]. CRF07_BC was distributed among IDUs in Xinjiang Province in northwestern China [2], while CRF08_BC was circulating widely among IDUs in Guangxi Province [1] and eastern part of Yunnan Province in southeastern China [4].

In the present study, we report the construction of the first replication-competent molecular clone of CRF08_BC and will discuss on its structural and biological properties.

## Materials and Methods

A CRF08_BC strain (00CN-HH040) was isolated from an IDU in Yunnan Province. The infectious molecular clone was reconstituted by PCR-based amplification-cloning method [5, 6], involving the direct ligation of 8.3-kb proviral amplicons into a recovery vector carrying two functional LTRs (Fig. 1). The infectivities to peripheral blood mononuclear cells (PBMCs) and primary macrophages and coreceptor usages were examined. The complete HIV-1 nucleotide sequence was determined and subjected to the recombination breakpoint analyses (bootscanning and informative site analyses) to verify the subtype structure.

## Results

### *Reconstitution and biological characterization of an infectious molecular clone of CRF08_BC*

An infectious molecular clone for CRF08_BC was isolated by two-

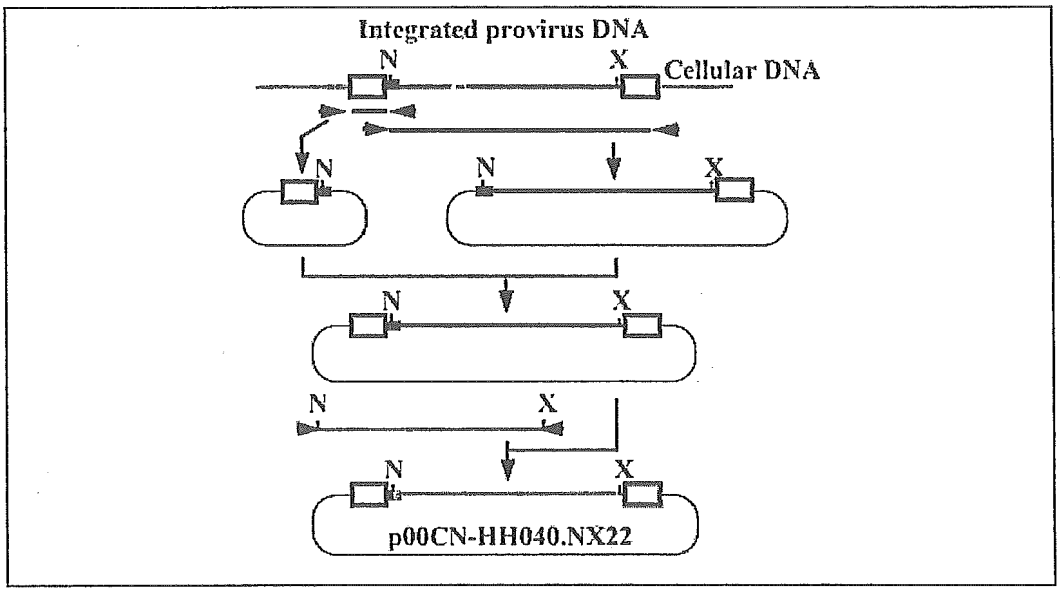


*Fig. 1. Schematic representation of the genetic reconstitution of infectious molecular clone of CRF08_BC (00CN-HH040.NX22).* Nar*I (N);* Xho*I (X).*

step reconstitution strategy, as illustrated in Fig. 1. We identified one clone, designated 00CN-HH040.NX22, that was capable of replicating in PHA/IL-2-stimulated PBMCs to high titers, comparable to parental primary isolate. This clone utilized CCR5 as a coreceptor for entry, but did not replicate in primary macrophages.

## *Structural characterization of infectious molecular clone 00CN-HH040.NX22*

The complete nucleotide sequence of 00CN-HH040.NX22 was determined to ensure that this clone indeed belongs to CRF08_BC. The phylogenetic tree analysis of the complete genome of 00CN-HH040.NX22 showed that it was clustered tightly with CRF08_BC reference strains with high bootstrap support (100%). The recombination breakpoint analyses (bootscanning and informative site analyses) corroborated that 00CN-HH040.NX22 shared identical structural profile with CRF08_BC reference strain (98CN006) (Fig.2).

## *Sequence signatures specific to CRF08_BC*

The nucleotide sequence signatures unique to CRF08_BC were identified in enhancer-promoter region in LTR. All known CRF08_BC (5 of 5) harbored three complete sets of NFκB sites in LTRs, which are common among most of subtype C family. 00CN-HH040.NX22 dis-

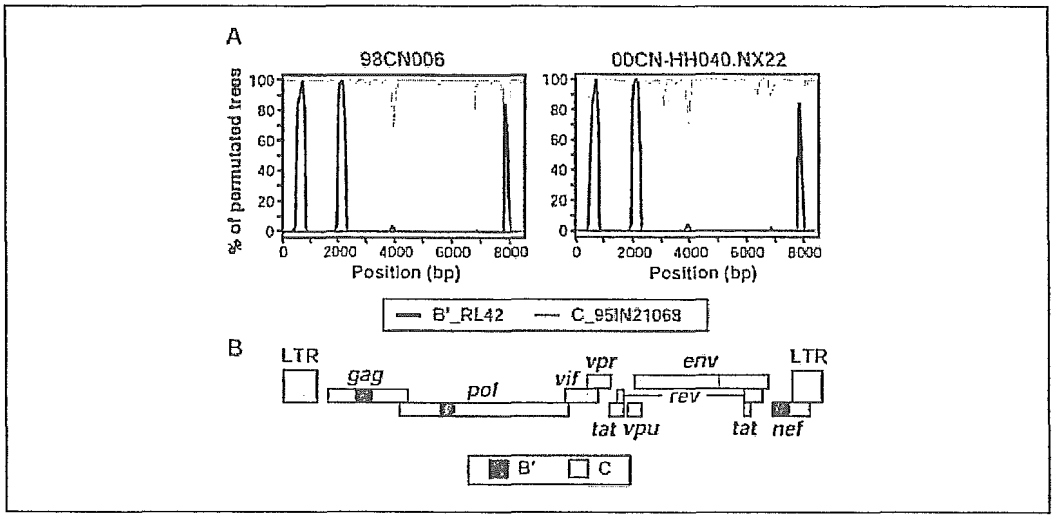


*Fig. 2. Recombinant structure of 00CN-HH040.NX22. (A) Bootscanning analyses of CRF08_BC reference strain (98CN006) (left) and 00CN-HH040.NX22 (right) with subtypes B' (RL42) and C (95IN21068) reference strains. subtype D (NDK) and CRF01_AE (93TH253) are used as distantly related references. The bootstrap values are plotted for a window of 500-bp moving in increments of 50-bp along the alignment. (B) Deduced subtype structure of 00CN-HH040.NX22.*

plays three-NF-κB configuration similar to other subtype C strains, but it harbors a C to T substitution in proximal NFκB binding motif in both 5' and 3' LTR regions. 00CN-HH040.NX22 retains the other sequence signature that appears to be specific to CRF08_BC [7]: *i.e.*, the spacer sequence between two distal NFkB sites (NFκB II and NFkB III) of 00CN-HH040.NX22 was comprised of two nucleotides (5'-GC-3'), similar to all known CRF08_BC strains (4 of 4) [7].

## Conclusions

In the present study, we described the structural and biological characterization of the first infectious molecular clone of CRF08_BC (00CN-HH040.NX22): This clone was reconstituted from primary HIV-1 CRF08_BC strain isolated from eastern part of Yunnan Province of China, where CRF08_BC is a principal circulating strain among IDUs [4]. This represents the first report of the isolation of a replication-competent HIV-1 molecular clone of CRF08_BC. It may facilitate the study to investigate the differences in the virological and immunological properties and to develop clade-specific molecular and immunological reagents. This clone may also be used for designing novel immunogens to limit the epidemic in southeastern China.

## References

1. PIYASIRISILP S, *et al.* A recent outbreak of human immunodeficiency virus type 1 infection in southern China was initiated by two highly homogeneous, geographically separated strains, circulating recombinant form AE and a novel BC recombinant. *J Virol* 2000,74:11286-11295.
2. SU L, *et al.* Characterization of a virtually full-length human immunodeficiency virus type 1 genome of a prevalent intersubtype (C/B') recombinant strain in China. *J Virol* 2000,74:11367-11376.
3. UNAIDS/WHO. AIDS epidemic update December 2001. 2001.
4. YANG R, *et al.* On-going generation of multiple forms of HIV-1 intersubtype recombinants in the Yunnan Province of China. *AIDS* 2002,16:1401-1407.
5. KUSAGAWA S, *et al.* Isolation and characterization of a full-lenght molecular DNA clone of Ghanaian HIV type 1 intersubtype A/G recombinant CRF02_AG, which Is replication competent in a restricted host range. *AIDS Res Hum Retroviruses* 2001,17:649-655.
6. KUSAGAWA S, *et al.* Isolation and characterization of replication-competent molecular DNA clones of HIV type 1 CRF01_AE with different coreceptor usages. *AIDS Res Hum Retroviruses* 2002,18:115-122.
7. YANG R, *et al.* Identification and characterization of a new class of human immunodeficiency virus type 1 recombinants comprised of two circulating recombinant forms, CRF07_BC and CRF08_BC, in China. *J Virol* 2003,77:685-695.

BRIEF REPORT

# Identification of Attenuated Variants of HIV-1 Circulating Recombinant Form 01_AE That Are Associated with Slow Disease Progression Due to Gross Genetic Alterations in the *nef*/Long Terminal Repeat Sequences

**Makiko Kondo,[1] Takako Shima,[1] Masako Nishizawa,[3] Koji Sudo,[1] Shinya Iwamuro,[2] Takeshi Okabe,[2] Yutaka Takebe,[4] and Mitsunobu Imai[1]**

[1]Division of Microbiology, Kanagawa Prefectural Institute of Public Health, and [2]Atsugi City Hospital, Kanagawa, and [3]AIDS Research Center, National Institute of Infectious Diseases, Musashimurayama, and [4]AIDS Research Center, National Institute of Infectious Diseases, Shinjuku-ku, Tokyo, Japan

**We identified an unusual case of human immunodeficiency virus type 1 (HIV-1) infection in a patient (GM43) who exhibited a persistently low antibody response and undetectable viral load during a 5-year follow-up period. GM43 harbored HIV-1 circulating recombinant form 01_AE with gross deletions in the *nef*/long terminal repeat (LTR) region. The sizes of the deletions increased progressively from 84 to >400 bp during the 5-year period. GM43 appeared to have acquired defective variants from her husband. The genetic alterations in the *nef*/LTR region were remarkably similar to those that have been reported in slow progressors (such as the slow progressors in the Sydney Blood Bank Cohort). The present study is the first report of slow disease progression due to gross genetic alterations in the *nef*/LTR region in a person infected with an HIV-1 non–subtype B strain.**

Rates of disease progression vary among individuals infected with HIV-1, because of the complex interplay between host genetic and immunologic factors and the pathogenic potential of the infecting virus. The viral *nef* gene is one of the crucial determinants of disease progression, as has been demonstrated in animal models [1–3]. That the *nef* gene is a key factor for disease progression in humans is strongly supported by the finding that some long-term nonprogressors (LTNPs) with low viral loads (despite 10–14 years of HIV-1 infection) carry viruses with gross deletions [4–6] or small structural defects and mutations [7] in the *nef* gene.

The *nef* gene is known to have pleiotropic functions, including down-regulation of the cell-surface expression of CD4 and class I major histocompatibility complex (MHC) molecules, enhancement of viral replication and infectivity, induction of cytokine and chemokine expression by T cells and macrophages, and blockage of proapoptotic signaling by HIV-1–infected cells (reviewed in Geyer et al. [8]). A large number of cellular interaction partners critical to *nef* gene functions have been identified, and the binding sites have been mapped to distinct locations within the Nef protein (reviewed in Geyer et al. [8]).

Although the genetic alterations in the *nef* gene that are associated with slow disease progression have been identified in HIV-1 subtype B in US and European populations [4–7], it remains unclear whether these alterations are found only in the subtype B lineage. In the present study, we identified attenuated variants of HIV-1 circulating recombinant form 01_AE (CRF01_AE) that harbored gross deletions in the *nef*/long terminal repeat (LTR) region in an asymptomatic patient (GM43) who had an unusually weak antibody response and an undetectable viral load during a 5-year follow-up period, demonstrating the association between *nef*/LTR deletions and slow disease progression with respect to infection with a non–subtype B strain.

***Patients, materials, and methods.*** Informed consent was obtained from the patients, and the study was conducted in accordance with the clinical research guidelines of Japan. Antibodies to HIV-1 were detected by use of the Serodia HIV-1 gelatin particle agglutination (PA) test (Fujirebio), and Western-blot (WB) analysis (LAV Blot I; Bio-Rad) was used for confirmation. Plasma HIV-1 RNA loads were measured by the ultrasensitive method with the Amplicor HIV-1 Monitor Kit (version 1.5; Roche Diagnostics), which allows the sensitive

Received 7 September 2004; accepted 9 February 2005; electronically published 25 May 2005.

Reprints or correspondence: Dr. Mitsunobu Imai, Div. of Microbiology, Kanagawa Prefectural Institute of Public Health, 1-3-1 Shimomachiya, Chigasaki-shi, Kanagawa 253-0087, Japan (imaim@d2.dion.ne.jp); or, Dr. Yutaka Takebe, Laboratory of Molecular Virology and Epidemiology, AIDS Research Center, National Institute of Infectious Diseases, Toyama 1-23-1, Shinjuku-ku, Tokyo 162-8640, Japan (takebe@nih.go.jp).

**The Journal of Infectious Diseases 2005; 192:56–61**

0022-1899/2005/19201-0010$15.00

Presented in part: XIV International AIDS Conference, Barcelona, Spain, 10 July 2002 (abstract WePeC6234).

Financial support: Grants from AIDS study groups sponsored by the Ministry of Health, Labor, and Welfare, Japan; Japanese Foundation for AIDS Prevention Research Resident Program (to K.S.).

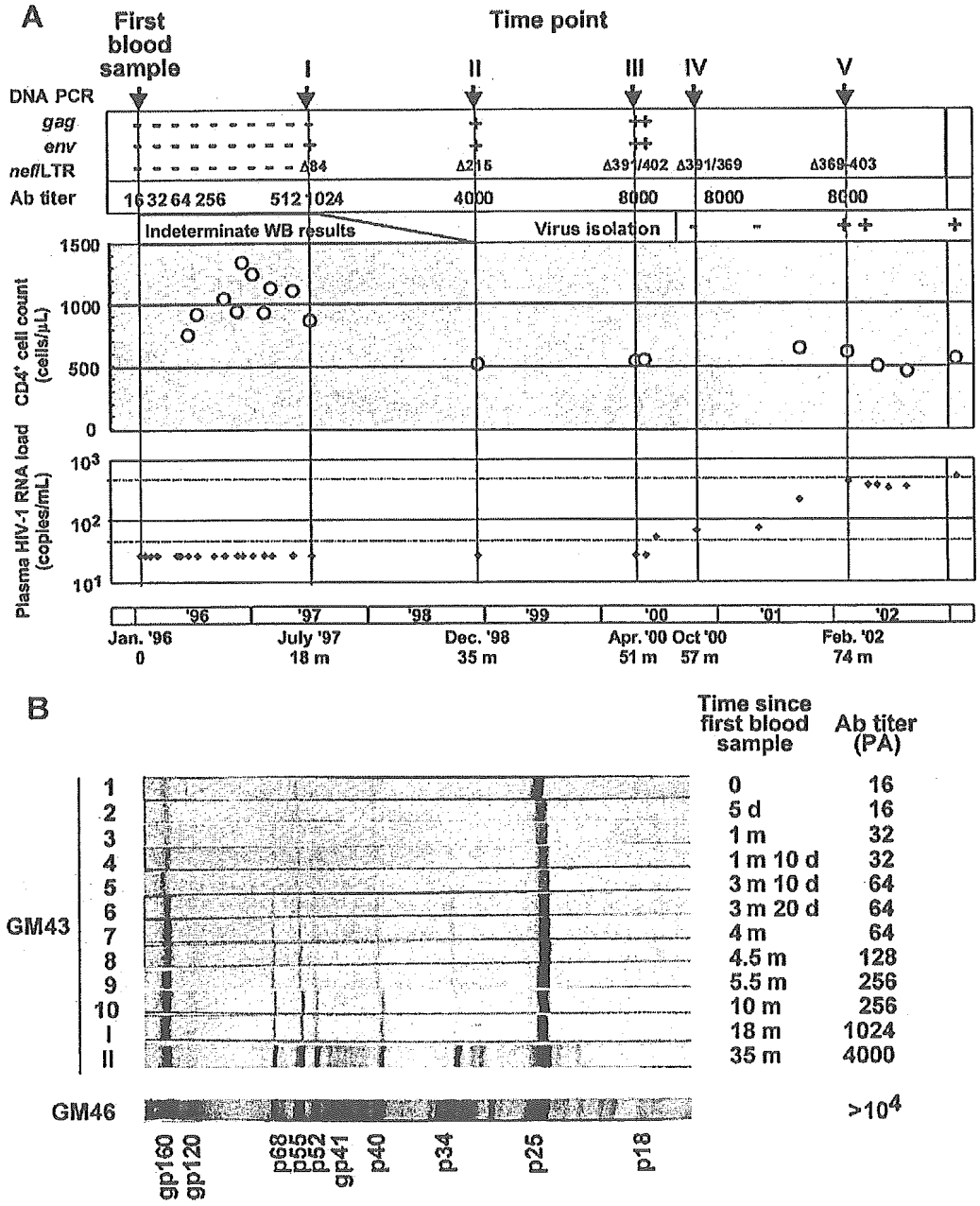


**Figure 1.** Changes in serological and virological parameters in patient GM43. *A*, Profiles of serological and virological parameters. *Top*, Detection of proviral HIV-1 DNA by nested polymerase chain reaction (PCR) for *gag* (p24), *env* (C2/V3), and the *nef*/long terminal repeat (LTR) region. Antibody (Ab) titers (determined by the Serodia HIV-1 gelatin particle agglutination [PA] test) are also shown. −, negative; +, positive; Δ, the size (in base pairs) of the deletion in the *nef*/LTR region in major PCR products; WB, Western blot. *Middle*, $CD4^+$ cell count, in cells per microliter of blood *(white circles)*. *Bottom*, Plasma HIV-1 RNA load, in copies per milliliter of blood (log scale) *(black diamonds)*. HIV-1 proviral genomes were analyzed by use of the serum samples collected at the indicated time points (I–V). HIV-1 was isolated from GM43 for the first time in February 2002 (time point V). *B*, WB analysis (LAV Blot I; Bio-Rad) for GM43 and her husband, GM46. Strips 1–10 are for serum samples serially collected between January and October 1996, and strips I and II are for serum samples collected in July 1997 (time point I) and December 1998 (time point II). d, day; m, month.

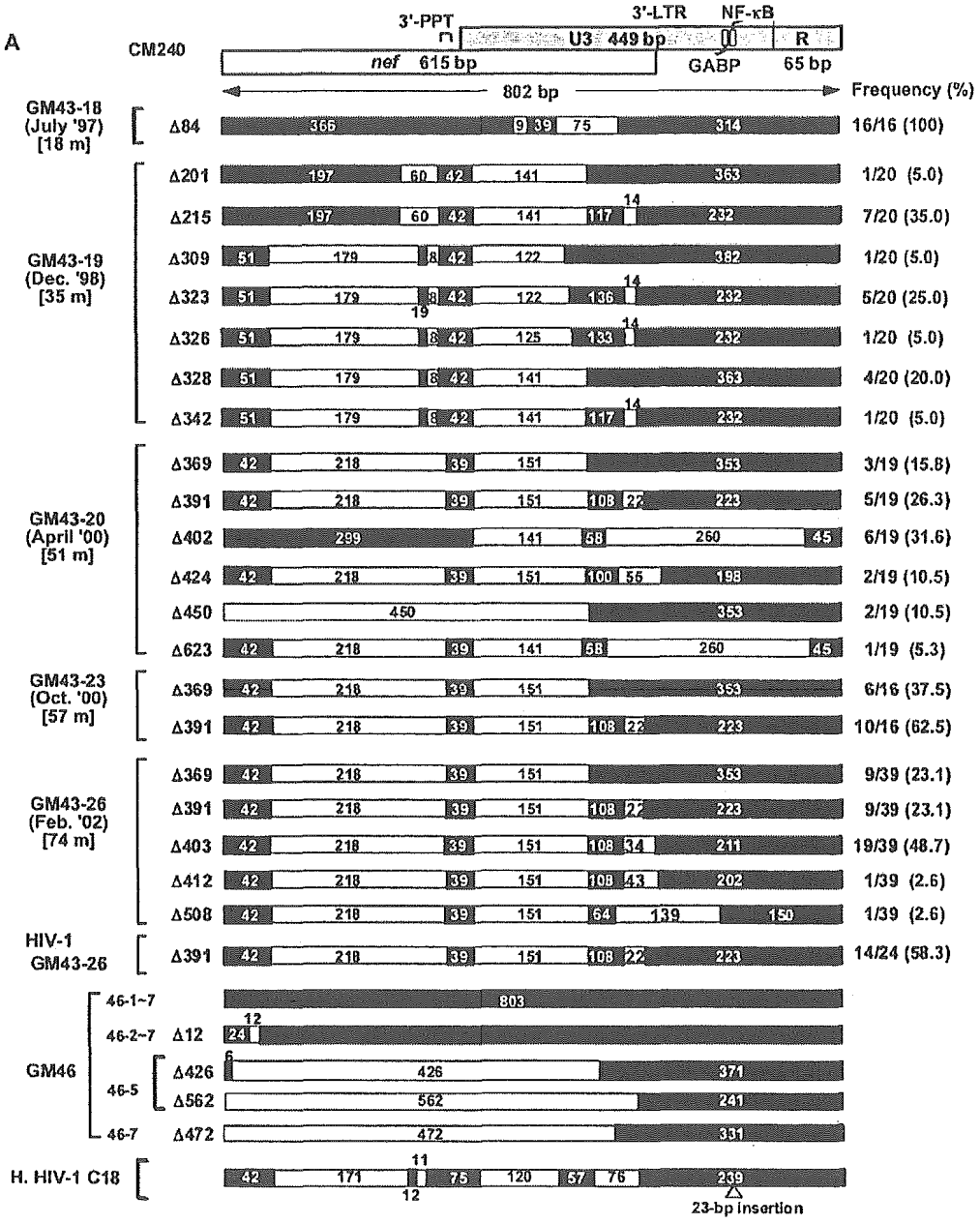


**Figure 2.** Genomic organization of the *nef*/long terminal repeat (LTR) region. *A*, Schematic drawing of the genomic structure of HIV-1 circulating recombinant form (CRF) 01_AE CM240 [12] for the corresponding region, at top. The genomic organizations of HIV-1 isolates from patient GM43 and her husband, GM46, and of HIV-1 variant C18 (an attenuated variant of HIV-1 subtype B detected in the Sydney Blood Bank Cohort [5]) are shown for comparison. Black bars represent amplified sequences, and white bars represent deletions. The nucleotide positions are shown relative to CM240. The numbers in the white bars represent the sizes of the deletions. m, month; PPT, polypurine tract. *B*, Comparison of the genetic organization of the *nef*/LTR region in GM43-20, a major quasispecies (Δ391) found in GM43, with that of C18 [5]. *C*, Sequence landmarks and the sites of deletions in the *nef*/LTR region in GM43-20. C18 carries a 23-bp duplication comprised of a single set of NF-κB and Sp1 sequences.

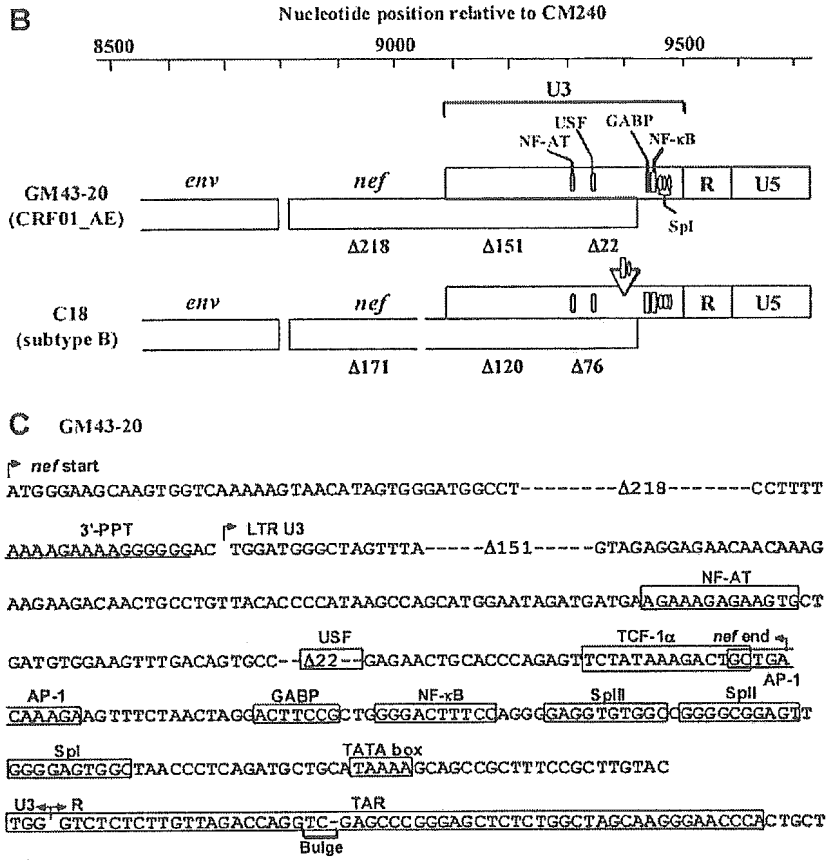


**Figure 2.** *(Continued.)*

detection of HIV-1 RNA from both HIV-1 subtype B and non–subtype B strains, including CRF01_AE [9]. Replication-competent HIV-1 strains were isolated by cocultivation with CD8-depleted peripheral-blood mononuclear cells (PBMCs) from healthy donors. PBMCs were activated by use of anti-CD3 antibody (CLB-CD3; PeliCluster), instead of the standard activation stimuli of phytohemagglutinin and interleukin-2, to improve the efficiency of isolation [10, 11].

The *nef*/LTR regions of HIV-1 provirus genomes were amplified by nested polymerase chain reaction (PCR), with the outer primers Env43F14 (sense; 5′-GAGTTAGGCAGGGATACTCAC-3′; positions 7892–7912 of the genome of CM240, the HIV-1 CRF01_AE reference strain [12]) and 3′LTR43R16 (antisense; 5′-TAAGCACTCAAGGCAAGC-3′; positions 9202–9185 of the genome of CM240) and the inner primers Env43F15 (sense; 5′-AGCCTGTGCCTCTTCAGCTACCA-3′; positions 8052–8083 of the genome of CM240) and MSR5 (antisense; 5′-GCACTCAAGGCAAGCTTTATTGAGGCT-3′; positions 9199–9173 of the genome of CM240). The nucleotide sequences of both strands were determined by the BigDye Terminator cycle sequencing method, using a Prism 310 DNA Sequencer (Applied Biosystems). Nucleotide sequences (GenBank accession numbers AB193797–AB193800) were aligned by use of CLUSTAL W (version 1.4). Phylogenetic trees were constructed by the neighbor-joining method, based on Kimura's 2-parameter distance matrix with 100 bootstrap replicates. Analyses were implemented by use of PHYLIP (version 3.573) [13].

*Results.* GM43 is a 28-year-old Thai woman who has lived in Japan for the past 6 years. GM43 was infected with HIV-1 via her husband, GM46. GM46 had contracted HIV-1 via heterosexual contact before 1995, presumably in Thailand. Both GM43 and GM46 remain healthy and do not have any clinical symptoms. There is no indication of HIV-2 infection. In January 1996, serologic tests conducted for GM43 at her 18th week of pregnancy (her first visit) showed low marginal HIV-1 seropositivity, with a PA antibody titer of 1:16 (figure 1*A*). Indeterminate WB results (1+ reactivity for gp160 only) persisted for GM43 throughout an 18-month observation period, whereas GM46 was unequivocally positive by WB (figure 1*B*). Empirically, in most HIV-1–infected patients, PA antibody titers

exceed $1:10^3$ within 2 weeks of seroconversion and reach $1:10^4$ one month after seroconversion. However, in GM43, low PA antibody titers ($<1:10^3$) persisted for 1.5 years, and it took >4.5 years until her PA antibody titer reached $1:10^4$ (figure 1*A*).

In parallel with this slow process of seroconversion, GM43's plasma HIV-1 RNA load was persistently below the limit of detection by PCR (<50 copies/mL) during a 4.5-year period (figure 1*A*). HIV-1 proviral DNAs were amplified by nested PCR for the *env* (C2/V3) region only in July 1997 and for both the *gag* (p17) and *env* (C2/V3) regions in December 1998 (figure 1*A*), providing conclusive evidence that GM43 was infected with HIV-1. During the first 3 years after seroconversion, GM43's $CD4^+$ cell count gradually decreased, from 1074 to 600 cells/$\mu$L, as her plasma HIV-1 RNA load gradually increased, but her $CD4^+$ cell count remained stable thereafter, at 400–600 cells/$\mu$L (figure 1*A*).

To investigate the mechanism of this unusual clinical course, we examined the structural features of the *nef*/LTR region that are known to be associated with slow disease progression [4–6]. The *nef*/LTR regions of HIV-1 proviral genomes were amplified by nested PCR from the PBMC DNAs sampled at 5 different time points between July 1997 and February 2002 (time points I–V, as shown in figure 1). Although the expected size of amplicons of the *nef*/LTR region of the intact HIV-1 genome is 1140 bp, the resulting amplified fragments ranged in size from 500 to 1000 bp, indicating the existence of deletions of ~100–500 bp in the *nef*/LTR region.

To further characterize the genetic alterations in the *nef*/LTR region for GM43, we molecularly cloned (by the TA cloning method) the PCR products and determined the nucleotide sequences of 16–39 independent PCR clones at each time point. Nucleotide-sequence alignment revealed progressive deletions in the *nef*/LTR region over time (figure 2). Plasma HIV-1 RNA load was detectable after the increased deletions in the *nef*/LTR region (time points III–V). A replication-competent HIV-1 strain (GM43-23) was isolated for the first time at time point V. The HIV-1 quasispecies with the 391-bp *nef*/LTR deletion ($\Delta$391) appeared to constitute a major functional (replication-competent) segment of the proviral population in GM43.

We next analyzed the structural characteristics of the HIV-1 genomes for GM46. We attempted to amplify the *nef*/LTR region by PCR at 7 time points (time points 46-1 through 46-7, as shown in figure 2*A*) between 1996 and 1997 (GM46 then dropped out of the follow-up). At all sampling points except the first (46-1), both full-sized and smaller-sized PCR products (containing deletions ranging in size from 12 to 472 bp) were amplified (figure 2*A*) in independent PCR amplification experiments. Although we were not able to establish the exact frequency of defective genomes in GM46, considerable proportions of the HIV-1 quasispecies in GM46 appeared to contain gross genetic alterations in the *nef*/LTR region, especially at later time points. In contrast, no appreciable defects in the *nef*/LTR region were detected among 73 other CRF01_AE–infected individuals (of both Japanese and Thai nationality) in Japan. Phylogenetic-tree analysis based on nucleotide sequences of *env* (C2/V3) and the *nef*/LTR region revealed that HIV-1 sequences from GM43 and GM46 formed a monophyletic cluster within CRF01_AE, with high bootstrap support (100% and 98%, respectively) (data not shown). Furthermore, this GM43/GM46 cluster was distinct from other CRF01_AE local control sequences sampled in the same geographical region. These findings strongly suggest that GM43 was indeed infected via her husband. However, none of the deletions detected in GM46 were identical to those detected in GM43 (figure 2).

The genetic organization of *nef*/LTR deletions detected in GM43 and GM46 are summarized in figure 2. Two large deletions were detected. The first large deletion was located in the amino-terminal half of the *nef* gene that does not overlap with the LTR sequences. The second large deletion was mapped to the *nef*/U3–overlapping region. One or 2 small, additional deletions followed the 2 large deletions. Most of the first large deletion removed the highly conserved acidic (EEEE) domain and $(Pxx)_4$ motif, which are essential for Nef function. However, the downstream deletions located in the *nef*/U3 region left intact the polypurine tract (3′-PPT), NF-$\kappa$B, and SpI binding sites and the TATA box (figure 2), which are indispensable for HIV-1 replication, as was reported in the previous studies of defective subtype B variants in US and European populations [4–6].

The overall structural configuration of the *nef*/LTR deletions found in the CRF01_AE variant infecting GM43 was remarkably similar to that of the attenuated HIV-1 variant C18 (which belongs to HIV-1 subtype B) detected in the Sydney Blood Bank Cohort [5] (figure 2*A* and 2*B*). Of note, the sequence features unique to CRF01_AE—including the GABP motif (5′-ACTTCCG-3′), a single NF-$\kappa$B [14], an unusual TATA box (5′-TAAAA-3′), and a 2-nt bulge in TAR stems (figure 2)—were detected in GM43. No appreciable direct repeats that may have caused the deletion in the *nef*/LTR region [6] were detected in GM43.

***Discussion.*** We have identified a unique case of CRF01_AE infection, in which a patient, GM43, experienced an unusually slow increase in HIV-1 antibody titers and had an undetectable viral load over a prolonged period of time. GM43 carried attenuated viral variants with a range of *nef*/LTR deletions that were similar to those found in LTNPs infected with HIV-1 subtype B [4–6]. The present study is the first report demonstrating the association between gross *nef*/LTR deletions and slow disease progression in a patient infected with a non–subtype B strain.

As can be seen in figure 2, striking similarities in the alteration of the *nef*/LTR region between subtype B and CRF01_AE were observed. The genetic alterations observed in the *nef*/LTR region of an attenuated subtype B variant detected in the Sydney

Blood Bank Cohort (isolate C18 [5]) and the CRF01_AE variants found in GM43 in the present study removed most of the sequence elements essential for Nef functions—including the highly conserved acidic (EEEE) domain that is required for the down-regulation of class I MHC molecules and the $(Pxx)_4$ motif mediating the interaction between Nef and signaling molecules—and placed downstream sequences out of frame (figure 2). Although a number of deletions were present in the *nef* region that overlapped U3 in the LTR region, none of these alterations affected *cis*-acting elements known to be critical for viral replication, including the 3′-PPT, the U3 terminal sequences, the TATA box, and the NF-$\kappa$B and SpI binding sites. This convergent manner of evolution of such genetic alterations in the *nef*/LTR sequences implies the presence of the strong selection pressures that maintain the replication capacities in defective HIV-1 genomes.

Phylogenetic-tree analysis demonstrated that GM43 acquired CRF01_AE from her husband, GM46. Interestingly, GM46 was also found to harbor unique sets of *nef*/LTR deletions, although the profiles of the deletions detected in GM46 were not identical to those detected in GM43 (figure 2). It is tempting to speculate that the defective genomes detected in GM43 may have evolved from a minor viral quasispecies carried by GM46 that was not detected in the present study or that was present only transiently at the time of transmission to GM43. If this is the case, the lack of selection for functional *nef* alleles in GM43 during transmission and/or establishment of infection from GM46 is rather surprising, because functional forms of *nef* alleles are quickly and efficiently selected for in rhesus monkeys infected experimentally with *nef*-defective simian immunodeficiency virus [1]. This suggests that, in certain patients, attenuated viral variants might have a selective advantage over HIV-1 strains with an intact *nef* allele. For instance, an efficient immune response may contribute to the selection of *nef*-defective viruses that could escape the cytotoxic T lymphocyte recognition that is critical to the effective control of viral replication [15]. In light of the identification of this unique case of CRF01_AE infection, a systematic search for the viral and host factors that influence disease progression may be warranted—especially in less-studied regions of the HIV-1 epidemic, such as in developing countries in Asia—with a slow increase in antibody titer used as a convenient marker.


## Acknowledgments

We thank the staffs of the participating clinics for their help and Dr. Shingo Kato for his valuable advice on virus isolation.


## References


1. Kestler HW 3rd, Ringler DJ, Mori K, et al. Importance of the nef gene for maintenance of high virus loads and for development of AIDS. Cell **1991**; 65:651–62.
2. Du Z, Lang SM, Sasseville VG, et al. Identification of a nef allele that causes lymphocyte activation and acute disease in macaque monkeys. Cell **1995**; 82:665–74.
3. Hanna Z, Kay DG, Rebai N, Guimond A, Jothy S, Jolicoeur P. Nef harbors a major determinant of pathogenicity for an AIDS-like disease induced by HIV-1 in transgenic mice. Cell **1998**; 95:163–75.
4. Kirchhoff F, Greenough TC, Brettler DB, Sullivan JL, Desrosiers RC. Absence of intact nef sequences in a long-term survivor with nonprogressive HIV-1 infection [see comments]. N Engl J Med **1995**; 332:228–32.
5. Deacon NJ, Tsykin A, Solomon A, et al. Genomic structure of an attenuated quasi species of HIV-1 from a blood transfusion donor and recipients [see comments]. Science **1995**; 270:988–91.
6. Salvi R, Garbuglia AR, Di Caro A, Pulciani S, Montella F, Benedetto A. Grossly defective nef gene sequences in a human immunodeficiency virus type 1-seropositive long-term nonprogressor. J Virol **1998**; 72:3646–57.
7. Casartelli N, Di Matteo G, Argentini C, et al. Structural defects and variations in the HIV-1 nef gene from rapid, slow and non-progressor children. AIDS **2003**; 17:1291–301.
8. Geyer M, Fackler OT, Peterlin BM. Structure-function relationships in HIV-1 Nef. EMBO Rep **2001**; 2:580–5.
9. Triques K, Coste J, Perret JL, et al. Efficiencies of four versions of the AMPLICOR HIV-1 MONITOR test for quantification of different subtypes of human immunodeficiency virus type 1. J Clin Microbiol **1999**; 37:110–6.
10. Spina CA, Prince HE, Richman DD. Preferential replication of HIV-1 in the CD45RO memory cell subset of primary CD4 lymphocytes in vitro. J Clin Invest **1997**; 99:1774–85.
11. Wong JK, Hezareh M, Gunthard HF, et al. Recovery of replication-competent HIV despite prolonged suppression of plasma viremia. Science **1997**; 278:1291–5.
12. Carr JK, Salminen MO, Koch C, et al. Full-length sequence and mosaic structure of a human immunodeficiency virus type 1 isolate from Thailand. J Virol **1996**; 70:5935–43.
13. Felsenstein J. PHYLIP (phylogeny inference package) version 3.5c. Seattle, WA: Department of Genetics, University of Washington, **1993**.
14. Verhoef K, Sanders RW, Fontaine V, Kitajima S, Berkhout B. Evolution of the human immunodeficiency virus type 1 long terminal repeat promoter by conversion of an NF-kappaB enhancer element into a GABP binding site. J Virol **1999**; 73:1331–40.
15. Mariani R, Kirchhoff F, Greenough TC, Sullivan JL, Desrosiers RC, Skowronski J. High frequency of defective nef alleles in a long-term survivor with nonprogressive human immunodeficiency virus type 1 infection. J Virol **1996**; 70:7752–64.

JOURNAL OF VIROLOGY, Aug. 2005, p. 10386–10396 Vol. 79, No. 16
0022-538X/05/$08.00+0 doi:10.1128/JVI.79.16.10386–10396.2005


# Influence of Glycosylation on the Efficacy of an Env-Based Vaccine against Simian Immunodeficiency Virus SIVmac239 in a Macaque AIDS Model

Kazuyasu Mori,[1,2,3]* Chie Sugimoto,[1,2,3] Shinji Ohgimoto,[4] Emi E. Nakayama,[5] Tatsuo Shioda,[5] Shigeru Kusagawa,[1] Yutaka Takebe,[1] Munehide Kano,[1] Tetsuro Matano,[6] Takae Yuasa,[7] Daisuke Kitaguchi,[7] Masaaki Miyazawa,[7] Yumiko Takahashi,[8] Michio Yasunami,[8] Akinori Kimura,[8] Naoki Yamamoto,[1] Yasuo Suzuki,[3,9] and Yoshiyuki Nagai[10]

*AIDS Research Center, National Institute of Infectious Diseases, Shinjuku-ku, Tokyo 162-8640,[1] Tsukuba Primate Research Center, National Institute of Biomedical Innovation, Tsukuba, Ibaraki 305-0843,[2] CREST, Japan Science and Technology Agency, Kawaguchi, Saitama 332-0012,[3] Microbiology and Genomics, Department of Genome Sciences, Kobe University School of Medicine, Kobe, Hyogo 650-0017,[4] Department of Viral Infections, Research Institute for Microbial Diseases, Osaka University, Suita, Osaka 565-0871,[5] Department of Microbiology, Graduate School of Medicine, The University of Tokyo, Bunkyo-ku, Tokyo 113-0033,[6] Department of Immunology, Kinki University School of Medicine, Osaka-Sayama, Osaka 589-8511,[7] Department of Molecular Pathogenesis, Division of Medical Science, Medical Research Institute, Tokyo Medical and Dental University, Chiyoda-ku, Tokyo 101-0062,[8] Department of Biochemistry, University of Shizuoka School of Pharmaceutical Sciences and COE Program in the 21st Century, Shizuoka, Shizuoka 422-8526,[9] and Toyama Institute of Health, Kosugi, Toyama 939-0363,[10] Japan*

Received 8 December 2004/Accepted 2 May 2005

**The envelope glycoprotein (Env) of human immunodeficiency viruses (HIVs) and simian immunodeficiency viruses (SIVs) is heavily glycosylated, and this feature has been speculated to be a reason for the insufficient immune control of these viruses by their hosts. In a macaque AIDS model, we demonstrated that quintuple deglycosylation in Env altered a pathogenic virus, SIVmac239, into a novel attenuated mutant virus (Δ5G). In Δ5G-infected animals, strong protective immunity against SIVmac239 was elicited. These HIV and SIV studies suggested that an understanding of the role of glycosylation is critical in defining not only the virological properties but also the immunogenicity of Env, suggesting that glycosylation in Env could be modified for the development of effective vaccines. To examine the effect of deglycosylation, we constructed prime-boost vaccines consisting of Env from SIVmac239 and Δ5G and compared their immunogenicities and vaccine efficacies by challenge infection with SIVmac239. Vaccination-induced immune responses differed between the two vaccine groups. Both Env-specific cellular and humoral responses were higher in wild-type (wt)-Env-immunized animals than in Δ5G Env-immunized animals. Following the challenge, viral loads in SIVmac239 Env (wt-Env)-immunized animals were significantly lower than in vector controls, with controlled viral replication in the chronic phase. Unexpectedly, viral loads in Δ5G Env-immunized animals were indistinguishable from those in vector controls. This study demonstrated that the prime-boost Env vaccine was effective against homologous SIVmac239 challenge. Changes in glycosylation affected both cell-mediated and humoral immune responses and vaccine efficacy.**

Primate lentiviruses, human immunodeficiency viruses (HIVs), and simian immunodeficiency viruses (SIVs) share common genetic and biological properties. As SIVmac, originally isolated from macaques in primate research centers in the United States, causes AIDS in macaques with remarkable similarities to HIV type 1 (HIV-1) infection in humans, this AIDS monkey model has been utilized to study vaccine development and the pathogenesis of HIV infection (for reviews, see references 10, 14, 17, 43, and 47).

HIV/SIV infection in the host consists of two phases, the primary infection and chronic infection. During the primary infection, extensive viral replication and dissemination of the infection occur. In chronic infection, viral replication continues for a long period, eventually leading to AIDS. Due to the host immune response against the infection, these two phases are separated by a set point at which the viral load reaches its lowest level. The viral loads of the set point and chronic infection are inversely correlated with the control of SIV/HIV infection and predict disease progression (25, 31); however, it remains unclear which host responses determine the viral loads of the set point and chronic infection. Nevertheless, virus-specific immune responses have been implicated in the host's control of the infection. Cellular immunity, such as that shown by cytotoxic T lymphocytes (CTL) and helper T cells, has been reported to correlate with the control of HIV/SIV infection (for reviews, see references 2, 24, 28, and 39). The role of the neutralizing antibody (NAb) in the control of infection and the

* Corresponding author. Mailing address: Tsukuba Primate Research Center, National Institute of Biomedical Innovation, 1 Hachimandai, Tsukuba, Ibaraki 305-0843, Japan. Phone: 81-29-837-2121. Fax: 81-29-837-0218. E-mail: mori@nibio.go.jp.

emergence of escape mutants has also been reported previously (7, 16, 51).

Despite these immune responses against HIV/SIV infection, humans and macaques fail to contain the infection due to the virus properties. HIV/SIV infects major target cells, such as $CD4^+$ T cells and macrophages, by binding viral envelope glycoproteins (Env) to cellular surface proteins and CD4 and chemokine receptors (CCR5, CXCR4, or others) on target cells (5, 32). Since viral entry consists of multiple steps (virion binding to these viral receptors, conformational change of Env, and fusion between the virion and the cellular membrane) and the critical parts of Env used in these steps are exposed only during each step, naturally generated antibodies are only partly effective in preventing HIV/SIV infection in their hosts (7, 8). Primary isolates can be neutralized to various degrees by HIV-infected patient serum but not by contemporaneous autologous samples. Consequently, escape mutants against preexisting NAb are selectively replicated (51). Thus, effective NAb is rarely induced in HIV/SIV infection (8, 10). This could partly explain the failure of Env-based vaccine trials against HIV-1 (8, 50).

The heavy glycosylation of Env is a unique feature of HIV/SIV that is distinctive from features of other enveloped viruses and is significantly related to their neutralization-resistant property (8, 29, 44). We therefore assumed that the insufficient immune containment of HIV/SIV might be due to heavy glycosylation in Env and that the removal of some glycans might allow the host to mount a protective immune response against the infection. Thus, we studied the influence of deglycosylation on the replication of SIVmac239 in a T-cell line and created a quintuple deglycosylation mutant of SIVmac239 (Δ5G), which has maximal removal of N-glycans at amino acid residues 79, 146, 171, 460, and 479 in Env and retains a replication capability similar to that of SIVmac239 in phytohemagglutinin-stimulated rhesus peripheral blood mononuclear cells (PBMCs) (36, 40). We then examined the infection of rhesus macaques with Δ5G; although Δ5G was replicated as extensively as SIVmac239 during the primary infection, the subsequent Δ5G infection was restricted to a level less than the detection sensitivity of a plasma viral load assay by 8 weeks postinfection (p.i.), in contrast to high chronic viral replication in SIVmac239 infection. Furthermore, an almost sterilizing immunity against SIVmac239 was induced in Δ5G-infected animals (36). Interestingly, another quintuple-deglycosylation-mutation strain with mutations at amino acid residues 146, 156, 184, 244, and 247 in Env was created (44) and was demonstrated to share common features with Δ5G in viral replication in animals and in functions as an attenuated vaccine (20). Since these two viruses share only one deglycosylation mutation and other mutations distributed differently in surface envelope protein gp120 (SU), these two studies suggest that heavily glycosylated Env determines the pathogenicity of HIV/SIV.

To dissect the mechanism for notable containment of Δ5G infection after primary infection, we hypothesized that the Env of Δ5G, a viral protein that differs from that in SIVmac239, might elicit protective immunity against SIVmac239, because deglycosylation in Env might alter antigenic properties such as B-cell and T-cell epitopes and enhance the protective immunity against SIVmac239. For this purpose, we immunized animals with Env of Δ5G (Δ5G Env) or Env of SIVmac239 (the wild type; wt Env), and examined the effect of these vaccinations against SIVmac239 infection.

## MATERIALS AND METHODS

**Generation of SU DNA vaccines.** DNA vaccine plasmids expressing SIV mac239 SU or Δ5G SU, pJWSUmac239 and pJWSUmacΔ5G, were constructed using the expression vector pJW4303 (45). To produce secreted SU efficiently, the native signal sequence in the SIVmac239 SU gene was replaced with the human tissue plasminogen activator signal in plasmid pJW4303, and a termination codon was created at the cleavage site for SU transmembrane (TM) protein (9). An SIVmac239 SU or Δ5G SU DNA sequence was amplified with a pair of primers, SUmacA (5′-TGT**GCTAGC**TATGTCACAGTCTTTTATGGTGTAC-3′) and SUmacB (5′-CC**AGGATCC**TATTACCTCTTCACATCTGTGGGGG C-3′). The SUmacA primer consisted of nucleotides (nt) 6923 to 6955 of the SIVmac239 sequence (GenBank accession number M33262) and the boldface nucleotides, which were changed to create a NheI site; primer SUmacB consisted of nt 8412 to 8381 and the boldface nucleotides, which were changed to create a BamHI site, and the underlined nucleotides, which generated tandem termination codons. The PCR-amplified fragments were digested with NheI and BamHI and cloned into the NheI- and BamHI-digested eukaryotic expression vector pJW4303 to yield pJWSUmac239 and pJWSUmacΔ5G. These plasmids were prepared using a Plasmid Mega kit (QIAGEN, Tokyo, Japan).

**Generation of Env vaccinia vaccines.** Recombinant vaccinia viruses expressing Env of SIVmac239 or Δ5G, WRvvmac239 or WRvvΔ5G, respectively, were constructed using a vaccinia virus WR strain (WRvv) as described previously (15). To excise the entire coding region of the *env* gene from the cloned SIV plasmid, BamHI and SmaI sites were introduced by in vitro mutagenesis at 5′- and 3′-end-flanking sites of the *env* gene, respectively. Primer B-6808 (5′-GAA AGAGAAGAAGGATCCCGAAAAAGG-3′) consisted of nt 6796 to 9822 and the underlined mutations of the BamHI site; S-9537 (5′-TATGAATACTCCC GGGAGAAACCC-3′) consisted of nt 9527 to 9550 and the underlined mutations of the SmaI site. DNA fragments containing the *env* gene of SIVmac239 or Δ5G were isolated by digesting the mutated plasmids with BamHI and SmaI and were cloned into the SmaI- and BamHI-digested vaccinia virus vector plasmid pNZ68K2. To transfer the *env* gene from a recombinant plasmid to WRvv, the standard homologous recombination method using CV-1 cells was performed. Env expression in the recombinant vaccinia virus was confirmed by immunoprecipitation. The function of Env was confirmed by CD4- and CCR5-dependent fusion activity. The recombinant Env-expressing vaccinia viruses obtained were propagated and titrated in CV-1cells. The two recombinant viruses were propagated with similar kinetics in CV-1 cells.

**Expression of SU-expressing plasmids and Env-expressing vaccinia virus in vitro.** CV-1 cells were transfected with equal amounts of the following SU-expressing plasmids: pJWSUmac239, pJWSUmacΔ5G, or the vector pJW4303. Secreted SU metabolically labeled with $^{35}S$ protein labeling mix (PerkinElmer, Boston, MA) in culture supernatant was concentrated, immunoprecipitated with plasma from SIVmac239-infected monkeys, and then analyzed by sodium dodecyl sulfate-polyacrylamide electrophoresis (SDS-PAGE) as described previously (40). To examine Env-expressing vaccinia viruses, CV-1 cells were infected with WRvvmac239, WRvvΔ5G, or WRvv at a multiplicity of infection of 10, metabolically labeled with $^{35}S$ protein labeling mix overnight, lysed, immunoprecipitated with plasma from SIVmac239-infected monkeys, and then analyzed by SDS-PAGE as described for the expression of SU-expressing plasmids.

**Animals, immunization, and challenge.** Twelve juvenile rhesus macaques from Myanmar or Laos that were seronegative for SIV, simian T-cell lymphotropic virus, B virus, and type D retroviruses were used. As the polymorphism of major histocompatibility complex (MHC) genes influenced cellular immune responses against SIV/HIV infection, MHC II haplotypes and alleles of the macaques were determined (data not shown). All animals were housed in individual cages and maintained according to the rules and guidelines for experimental animal welfare stated by the National Institute of Infectious Diseases. As shown in Fig. 1, the 12 animals were divided into three immunization groups of four animals each: the SIVmac239 (wt)-Env immunization group (Mm0005, Mm0007, Mm0010, Mm0012), the Δ5G Env immunization group (Mm0001, Mm0002, Mm0003, Mm0009), and the vector control immunization group (Mm0004, Mm0006, Mm0008, Mm0011). All animals were inoculated with 1 mg of plasmid DNA in 1 ml of saline, one into each quadriceps femoris at 0, 4, and 8 weeks after the initial prime immunization (weeks p.p.). The boost consisted of $5 \times 10^7$ PFU of vaccinia virus in 1 ml of phosphate-buffered saline (PBS), administered in two 0.1-ml intradermal inoculations, one into the skin of each femur, and two 0.4-ml inoculations, one into each quadriceps femoris at 21 weeks p.p. All animals were

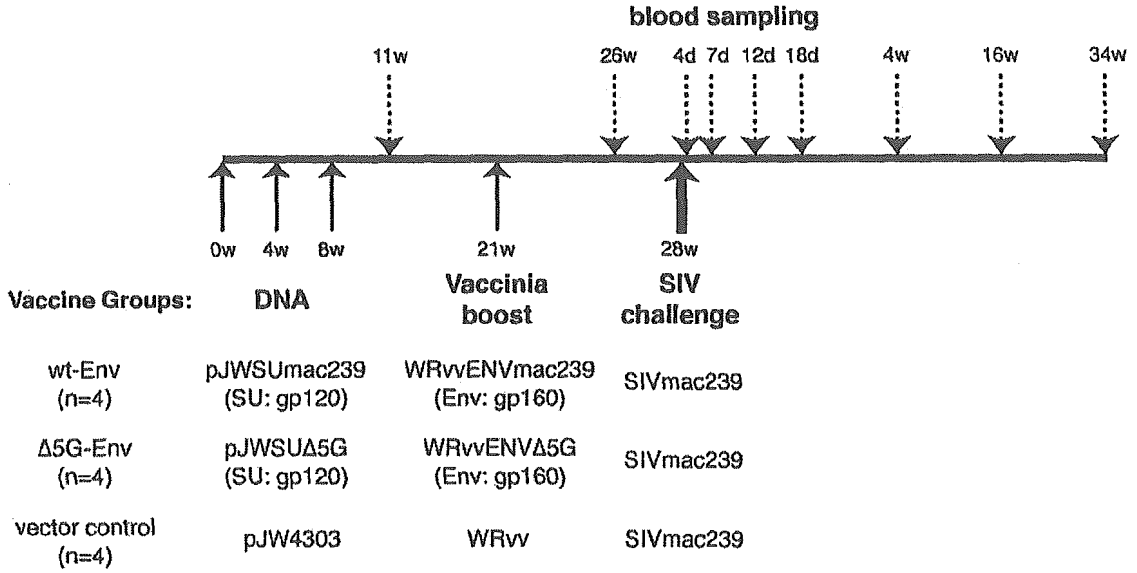


FIG. 1. Outline of immunization, challenge infection, and blood sampling. Twelve juvenile rhesus macaques were divided into three immunization groups of four animals each: the wt-Env immunization group (Mm0005, Mm0007, Mm0010, and Mm0012), the Δ5G Env immunization group (Mm0001, Mm0002, Mm0003, and Mm0009), and the vector control immunization group (Mm0004, Mm0006, Mm0008, and Mm0011). Animals were inoculated with a DNA vaccine (pJWSUmac239 for the wt-Env vaccine group, pJWSUΔ5G for the Δ5G Env vaccine group, and pJW4303 for the vector control group) at 0, 4, and 8 weeks p.p. The boost vaccine consisted of vaccinia virus (WRvvENVmac239 for the wt-Env vaccine group, WRvvENVΔ5G for the Δ5G Env vaccine group, and the WR strain for the vector control group) administered at 21 weeks p.p. All animals were challenged with 10 $TCID_{50}$ of SIVmac239 intravenously at 28 weeks p.p. w, weeks; d, day.

challenged with 10 50% tissue culture infective doses ($TCID_{50}$) of SIVmac239 intravenously at 28 weeks p.p.

**Viral load measurement.** To monitor SIV infection, the plasma viral load was measured by the real-time-PCR method described previously (36). Viral RNA was isolated from plasma from the infected animals using a commercial viral-RNA isolation kit (PE Applied Biosystems, Urayasu, Japan). SIV *gag* RNA was amplified and quantified using a commercial RNA reverse transcription (RT)-PCR kit (TaqMan EZ RT-PCR; PE Applied Biosystems) with the two *gag* primers, namely, the forward primer 1224F (5′-AATGCAGAGCCCCAAGAA GAC-3′), the reverse primer 1326R (5′-GGACCAAGGCCTAAAAAACCC-3′), and TaqMan probe 1272T (6-carboxyfluorescein-5′-ACCATGTTATGGCC AAATGCCCAGAC-3′-6-carboxymethylrhodamine). Purified viral RNA (10 μl) was reverse transcribed and amplified in a MicroAmp optical 96-well reaction plate (PE Applied Biosystems) according to the manufacturer's instructions and with the following thermal cycle conditions: 1 cycle of three sequential incubations (50°C for 2 min, 60°C for 30 min, and 95°C for 5 min) and then 50 cycles of amplification (95°C for 5 s, 62°C for 30 s) in a 7000 Prism sequence detection system (PE Applied Biosystems). In vitro RNA transcripts were quantified by optical density at 260 nm ($OD_{260}$) measurement and branched DNA assay for SIV viral RNA (Bayer Diagnostics, Tarrytown, N.Y.). RNA equivalent to 10 to $10^7$ copies per reaction was used as the standard for each assay. The detection sensitivity of plasma viral RNA using this method was 1,000 copies/ml.

**Flow cytometry.** CD4 depletion was monitored by measuring the percentage of $CD4^+$ T cells, memory cells ($CD29^{high}$ $CD4^+$) T cells (48) in PBMCs. PBMC samples were purified from a citrate anticoagulant containing blood using standard Ficoll-Hypaque gradient centrifugation. For flow cytometry, $2 \times 10^5$ PBMCs were reacted with fluorescein isothiocyanate or phycoerythrin-labeled antibodies (anti-human CD4, Nu-Th/I [Nichirei, Tokyo, Japan]; anti-human CD8, Leu2a [Becton Dickinson, San Jose, CA]; anti-human CD29, 4B4 [Coulter, Miami, FL]; anti-monkey CD3, FN-18 [Biosource, Camarillo, CA]; and anti-human CD20, Leu16 [Becton Dickinson, San Jose, CA]) as previously described (36, 37, 48).

**Peptides.** Overlapping peptides were synthesized by Emory University, Microchemical Facility, Winship Cancer Center (Atlanta, GA.). All SIVmac239 viral proteins except Env, Gag, Pol, Vif, Vpr, Vpx, Tat, Rev, and Nef were covered by consecutive 20-mer peptides overlapped by 12 amino acids. Env of SIVmac239 was covered by 72 consecutive 25-mer peptides overlapped by 13 amino acids. Peptides were dissolved in PBS with 10% dimethyl sulfoxide (Sigma Chemical, St. Louis, Mo.).

**rSeV.** Recombinant Sendai viruses (rSeV) expressing SIVmac239 Gag, SU, or Δ5G SU were used to infect herpesvirus papio-transformed B-lymphoblastoid cell lines (B-LCLs) to prepare autologous B-LCLs presenting these viral antigens. rSeV Gag expressing unprocessed SIVmac239 Gag and p55 (22, 23) and rSeV SU and rSeV/Δ5G SU expressing wt SU and Δ5G SU were constructed as described previously (52) and were also used to infect autologous B-LCLs.

**Anti-SIV ELISA.** A 1:100 dilution of each plasma sample in PBS (pH 7.4) containing a blocking reagent (Dainippon Seiyaku, Osaka, Japan) was assayed for SIV-specific antibody by using a standard enzyme-linked immunosorbent assay (ELISA) technique with 96-well plates precoated with SIVmac239 virion lysate. The $OD_{492}$ was measured using a microplate reader (range of absorbance with linearity, 0 to 3.0; Tecan Japan, Tokyo, Japan) and utilized as a relative measurement of the antibody titer.

**ELISPOT assay.** Virus-specific $CD4^+$ T cells and $CD8^+$ T cells in PBMCs were measured using a monkey γ-IFN ELISPOT assay kit (U-CyTech, Utrecht, The Netherlands).

Cryopreserved PBMCs were thawed and cultured overnight in R-10 medium (RPMI 1640 [Sigma] supplemented with 10% heat-inactivated, defined fetal bovine serum [HyClone, Logan, Utah], 55 μM 2-mercaptoethanol, 50 U/ml penicillin, and 50 μg/ml streptomycin). PBMCs were subjected to the depletion of $CD4^+$ cells with magnet beads coated with anti-human CD4 Ab (Dynal ASA, Oslo, Norway) or subjected to the depletion of $CD8^+$ cells with magnet beads coated with anti-human CD8 Ab (Miltenyi Biotec, Bergisch Gladbach, Germany). Depletion of $CD4^+$ or $CD8^+$ cells from PBMCs was confirmed by flow cytometry. Using this depletion method, more than 95% of $CD4^+$ or CD8 cells were removed from PBMCs. These PBMCs were used for ELISPOT assay for virus-specific $CD8^+$ T cells and virus-specific $CD4^+$ T cells. Virus-specific stimulation of T cells was performed with autologous B-LCLs pulsed with pooled peptides for Pol, Vif, Vpx, Vpr, Tat, Rev, and Nef or B-LCLs infected with an rSeV for Gag, wt Env, and Δ5G Env. B-LCLs were incubated with pooled peptides corresponding to each viral protein at a final concentration of 2 μg/ml or infected with rSeV at a multiplicity of infection of 10 at 37°C overnight. Peptide-pulsed or infected B-LCLs were inactivated with long-wave UV irradiation (19) in the presence of 10 μg/ml psoralen (Sigma) for 10 min at a distance of 3.5 cm from a UV light, washed three times with R-10, and then used as stimulators in an ELISPOT assay. $CD4^+$ or $CD8^+$ cell-depleted PBMCs were cultured with these stimulators in an anti-γ-IFN Ab-coated ELISPOT plate (U-CyTech) overnight according to the protocol for the kit. Spots on the ELISPOT plate were imaged using an Olympus model SZX12 microscope

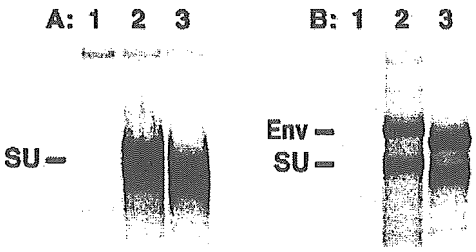


FIG. 2. Expression of SU and Env by SU-expressing DNA vaccines and Env-expressing vaccinia viruses. A: SU secreted in supernatant from CV-1 cells transfected with SU-expressing plasmids. Lane 1, pJW4303 vector; lane 2, pJWSUmac239; lane 3, pJWSUmacΔ5G. B: Env in cell lysates of CV-1 cells infected with recombinant vaccinia viruses. Lane 1, WRvv; lane 2, WRvvmac239; lane 3, WRvvΔ5G.

(Olympus, Tokyo, Japan) equipped with a digital camera, PDMCIe/OL (Polaroid, Cambridge, MA), and analyzed using a personal computer with MAC SCOPE version 2.61 (Mitani Corporation, Toyama, Japan). The results were calculated as numbers of spot-forming cells (SFC) per million PBMCs after subtraction of the background.

**Neutralization assay.** The original protocol of this neutralization assay was reported by Means et al. (29). Plasma that was heat inactivated at 56°C for 30 min was serially diluted and incubated with a fixed concentration of SIVmac239, Δ5G, or a macrophage-tropic SIV, 239/envMERT, at room temperature for 1 h. CEMx174/SIVLTR-SEAP cells were added to the mixture and then incubated at 37°C for 3 days. Secreted alkaline phosphatase activity in the culture supernatant was measured using a Phospha-Light System (Applied Biosystems). Chemiluminescence was detected with a Wallac Microbeta plate reader.

**Statistical analysis.** Statistical analysis was based on the Mann-Whitney test and performed using GraphPad Prism 4.0 software.

## RESULTS

**Experimental design.** We adopted a DNA prime-vaccinia virus boost regimen to immunize rhesus macaques with wt Env or Δ5G Env as shown in Fig. 1. Twelve macaques were immunized at 0, 4, and 8 weeks after the initial prime immunization (weeks p.p.) with one of three different DNA expression plasmids ($n = 4$): pJWSUmac239 expressing SU of SIVmac239, pJWSUΔ5G expressing SU of Δ5G, or the vector pJW4303. At 21 weeks p.p., all animals were boosted with recombinant WR vaccinia viruses expressing the respective Env proteins: vaccinia virus expressing Env of SIVmac239, vaccinia virus expressing Env of Δ5G, or vaccinia virus (Fig. 1).

**Expression of SU DNA plasmids and Env vaccinia viruses in vitro and in animals.** Although Δ5G replicated similarly to wild-type SIVmac239 in animals (36), quintuple deglycosylation might affect the expression of SU in a plasmid vector and the expression of Env in the vaccinia virus vector. Thus, we examined the expression of these vaccines in CV-1 cells. SU expressions in the wild-type plasmid (pJWSUmac239) and in the deglycosylated SU plasmid (pJWSUmacΔ5G) were at similar levels (Fig. 2A). The expression and processing of Env in the wild type (WRvvENVmac239) and in the deglycosylated Env mutant vaccinia virus (WRvvENVΔ5G) were also at similar levels (Fig. 2B). The reduced molecular size of the proteins due to deglycosylation was confirmed by PAGE (Fig. 2). As the amount of secreted SU in the supernatant by DNA transfection was comparable to that of Env in the cell lysate from CV-1 cells infected with WRvvEnv, a high expression of SU was achieved in a *rev*-independent manner by the pJW403 expression plasmid as described previously (9).

The expression of Env vaccines in the immunized animals was indirectly estimated by Env-specific antibody responses measured by a peptide ELISA using overlapping Env peptides. Env peptide-specific Ab was detected from 11 weeks p.p. after immunization with DNA vaccines, whereas there was no significant difference in the titers and the specificity of the responses between the two vaccine groups (data not shown), suggesting similar amounts of Env expressed in animals immunized with either Env vaccine. To examine the protective effect of the Env vaccines, all animals were challenged with 10 $TCID_{50}$ of SIVmac239 intravenously at 28 weeks p.p.

**Cellular immune responses elicited by Env vaccines.** The DNA prime-vaccinia virus boost regimen has been used in many studies, has successfully induced a high frequency of virus-specific $CD8^+$ T cells in macaques, and has conferred protective immunity against chimeric simian/human immunodeficiency virus (SHIV) (3, 27, 45). We therefore examined the vaccine-induced Env-specific T-cell responses by IFN-γ ELISPOT assay. Since deglycosylation in Env might change T-cell epitopes in SIVmac239, we measured the wt-SU and Δ5G SU-specific T-cell response by using autologous B-LCLs infected with recombinant Sendai viruses expressing either wt SU and/or Δ5G SU, respectively.

Although there was a tendency for more ELISPOT-positive cells to be observed by homologous SU than heterologous SU, comparable results were obtained by both assays (Fig. 3A and B). As vaccinated animals were challenged with SIVmac239, the results from the wt-SU assay were subsequently used to assess the SU-specific immune response. Immunization with the DNA vaccine induced only marginal SU-specific $CD8^+$ T cells or $CD4^+$ T cells at 11 weeks p.p.; however, boost immunization with recombinant WR vaccinia virus significantly increased SU-specific $CD8^+$ T cells and $CD4^+$ T cells in PBMCs at 26 weeks p.p. (Fig. 3A, B, and C). Notably, SIVmac239 Env (wt Env) induced twofold more SU-specific CD8 T cells (mean, 770 SFC per million PBMCs; range, 540 to 880) responding to wt SU than Δ5G Env (mean, 320; range, 110 to 400) ($P = 0.029$) (Fig. 3A and C). Similarly, twofold more SU-specific $CD4^+$ T cells were observed in wt-Env vaccinees (mean, 1,260; range, 840 to 1,710) than in Δ5G Env vaccinees (mean, 680; range, 150 to 1,260) at 26 weeks p.p. ($P = 0.11$) (Fig. 3B and C). Thus, a twofold-greater number of both SU-specific $CD4^+$ T cells and $CD8^+$ T cells were induced in SIVmac239 Env vaccinees than in Δ5G Env vaccinees at 26 weeks p.p. In vector controls, only negligible SU-specific $CD4^+$ T cells and $CD8^+$ T cells were detected in PBMCs at 26 weeks p.p. (Fig. 3A and B).

**Humoral immune response elicited with Env vaccines.** The anti-Env Ab titer was examined by SIVmac239 virion lysate ELISA. Anti-SIV Ab was detected in both wt-Env vaccinees and Δ5G Env vaccinees after an rVV boost (Fig. 4) (26 weeks p.p.). Anti-SIV Ab titers were comparable between the two vaccine groups.

Next, we examined the NAb against either SIVmac239, Δ5G, or a macrophage-tropic mutant, 239env/MERT (33, 35), in the two vaccine groups. Macrophage-tropic SIVs were highly susceptible to neutralization by plasma from most SIV-infected macaques (29), whereas SIVmac239 was highly resistant to neutralization as were most clinical isolates of HIV-1

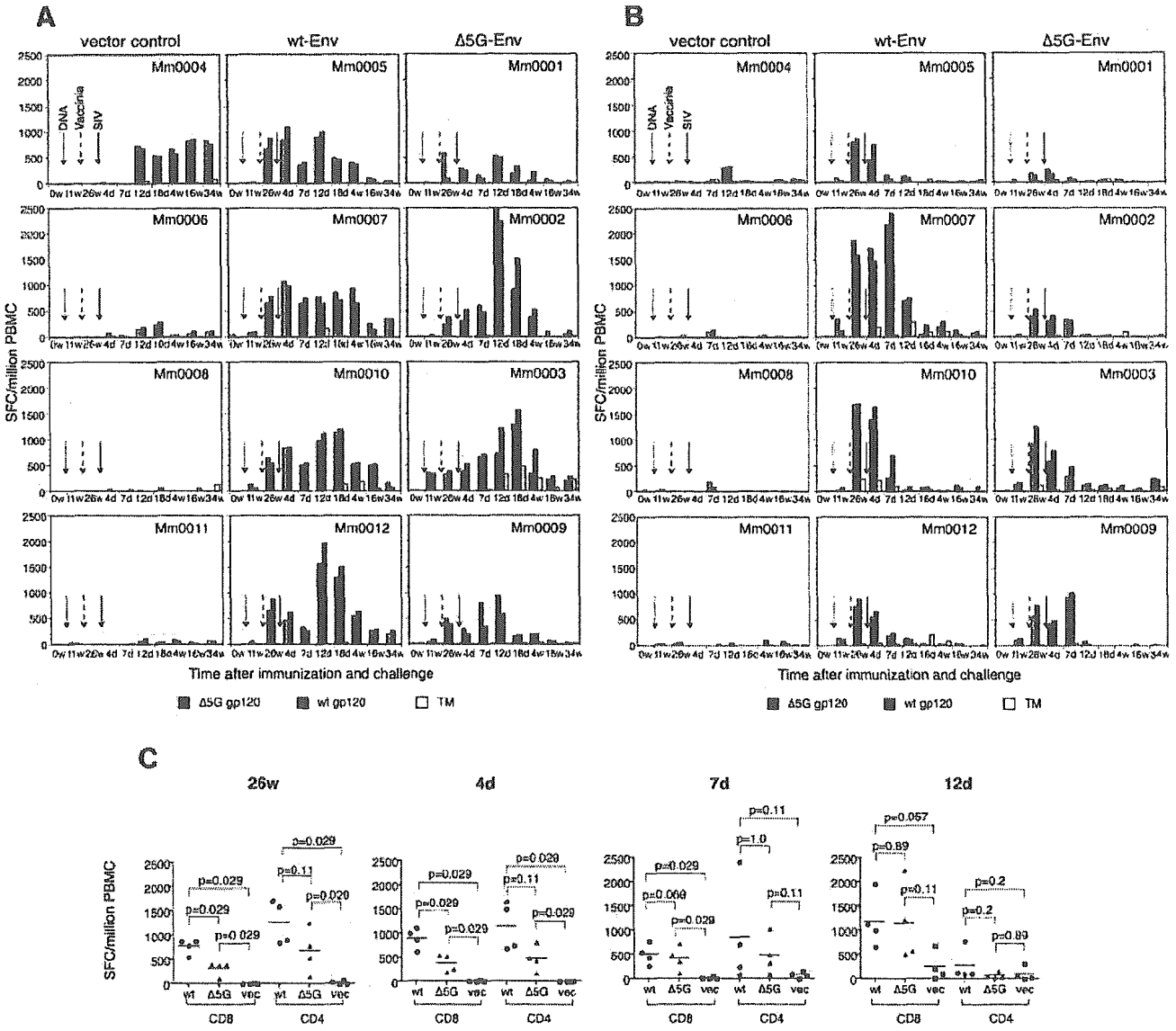


FIG. 3. Env-specific $CD4^+$ T-cell and $CD8^+$ T-cell responses in 12 macaques. A: Env-specific $CD8^+$ T cells in PBMCs were measured by ELISPOT assay for IFN-γ in three groups. B: Env-specific $CD4^+$ T cells in PBMCs were measured by ELISPOT assay for IFN-γ in three groups. ELISPOT results are colored as follows: Δ5G SU-specific T cells (red), wt-SU-specific T cells (green), and TM-specific T cells (yellow). Arrows with a dotted line, arrows with broken line, and arrows with a solid line indicate the time of the third DNA vaccination at 8 weeks p.p., the time of the vaccine boost at 21 weeks p.p., and the time of SIVmac239 challenge at 28 weeks p.p., respectively. C: Comparison of SU-specific $CD8^+$ T cells and $CD4^+$ T cells in PBMCs among the wt-Env vaccine group, the Δ5G Env vaccine group, and the vector control group at 26 weeks p.p. and 4, 7, and 12 days p.i. The numbers of SFC responding to SIVmac239 SU were used to compare the effects of the two vaccines. w, weeks; d, days.

(21, 29, 30). Plasma at 26 weeks p.p. from all immunized animals failed to neutralize not only SIVmac239 but also a multiple-deglycosylation-mutation strain, Δ5G (Table 1); in contrast, these plasma specimens did neutralize 239env/MERT. Furthermore, a marked difference was observed between the two vaccine groups. The NAb titer in the wt-Env vaccine group was eightfold higher than in the Δ5G Env vaccine group (Table 1). The difference of this immune response between the two vaccine groups was significant ($P = 0.029$).

**SIV replication in Env-immunized animals.** As described above, wt-Env vaccine and Δ5G Env vaccine induced different magnitudes of virus-specific cellular and humoral immunity in macaques. To examine the effect of the two vaccines, we challenged the vaccinated animals with SIVmac239. Viral loads in vector controls were mostly consistent with our previous results with SIVmac239-infected rhesus macaques (36, 48). The mean peak viral load at 2 weeks p.i. was $1.4 \times 10^7$ copies/ml, with a range of $0.5 \times 10^7$ to $2.2 \times 10^7$ copies/ml. Viral loads in chronic infection diverged into two patterns (Fig. 5A). Subsequent to the set point at 20 weeks p.i., the viral loads in three animals increased more than $10^4$ copies/ml. In contrast, viral loads in one animal (Mm0011) remained as low as 1,000 copies/ml up to 45 weeks p.i.

Compared with the vector controls, viral loads in wt-Env

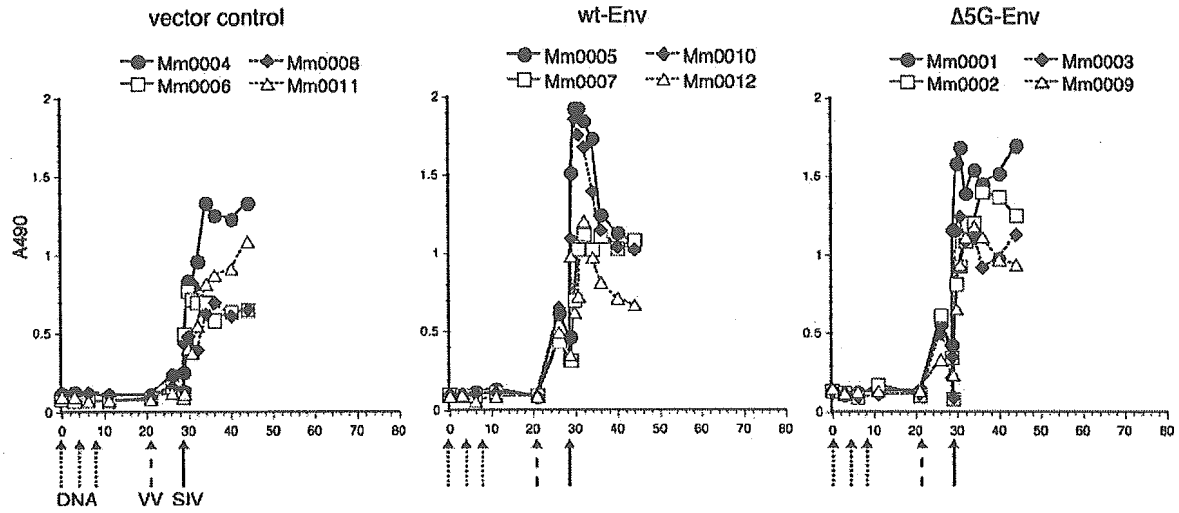


FIG. 4. Humoral immune response during immunization and after challenge infection. The $OD_{492}$ was used as a relative measurement of anti-SIV ELISA antibody titer.

vaccinees were markedly reduced (Fig. 5B). Peak viral loads at 2 weeks p.i. (mean, $1 \times 10^6$ copies/ml; range, $0.8 \times 10^5$ to $1.2 \times 10^6$ copies/ml) were 1-log lower than those in the vector controls. Furthermore, viral loads decreased to as low as 1,000 copies/ml by 8 to 20 weeks p.i., remaining low until autopsy at 45 weeks p.i.

Unexpectedly, viral loads in the Δ5G Env vaccine group resembled those in vector controls (Fig. 5C). Peak viral loads (mean, $2.4 \times 10^6$ copies/ml; range, $0.9 \times 10^6$ to $4.2 \times 10^6$ copies/ml) were slightly lower than those in vector controls. Set points and viral loads in the chronic phase were similar to those of vector controls.

In summary, as shown by the mean viral loads in primary and chronic infection (Fig. 5D) and statistical analysis (Fig. 5E), the effects of vaccination differed between the wt-Env vaccine and Δ5G Env vaccine. In the effect on primary infection (up to 6 weeks p.i.), wt-Env vaccination decreased viral loads more extensively and significantly than Δ5G Env vaccination ($P$ = 0.029 versus $P$ = 0.057); however, in chronic infection (viral loads after 8 weeks p.i.), significant reductions in viral loads compared with those in vector controls were seen only in the wt-Env vaccine group and not the Δ5G Env vaccine group (Fig. 5E). Collectively, wt-Env vaccination induced significantly effective immunity to control SIVmac239 infection, whereas Δ5G Env vaccination induced a marginal effect seen only in primary and not in chronic infection.

TABLE 1. Neutralizing-antibody titers in the vaccinated macaques at 26 weeks p.p.

| Vaccine | Animal | Neutralizing-antibody titer[a] | | | Mean[b] |
|---|---|---|---|---|---|
| | | SIVmac239 | Δ5G | 239/envMERT | |
| wt-Env | Mm0005 | <20 | <20 | 800 | |
| | Mm0007 | <20 | <20 | 400 | |
| | | | | | 400 |
| | Mm0010 | <20 | <20 | 400 | |
| | Mm0012 | <20 | <20 | 200 | |
| Δ5G-Env | Mm0001 | <20 | <20 | 100 | |
| | Mm0002 | <20 | <20 | 20 | |
| | | | | | 50 |
| | Mm0003 | <20 | <20 | 100 | |
| | Mm0009 | <20 | <20 | 50 | |

[a] Reciprocal of the dilution of plasma giving 50% inhibition of SIV replication.
[b] The difference in NAb levels between the two vaccine groups was significant ($P$ = 0.0029).

**$CD4^+$ T-cell subsets in PBMCs.** CD4 cell depletion is a primary manifestation indicating immune disorder in HIV/SIV infection. As CD4 depletion results from HIV/SIV infection in lymphatic tissue, it correlates with the extent of viral replication. Accordingly, viral loads were correlated mostly with CD4 depletion (Fig. 5 and 6A). Despite fluctuations due to immunizations and the challenge infection, the percentage of $CD4^+$ T cells in wt-Env-immunized animals in the chronic phase recovered to the levels at the initiation of the experiment. By contrast, in vector controls and Δ5G Env vaccinees, the percentage of $CD4^+$ T cells decreased in the chronic phase. Among them, an extensive decrease in $CD4^+$ T cells occurred in animals with high viral loads in the chronic phase (Mm0001, Mm0008, and Mm0009) (Fig. 5 and 6A). However, in the other animals, the levels of $CD4^+$ T cells remained as before the challenge (Mm0003, Mm0011).

A subset of $CD4^+$ CD29 high cells, approximately corresponding to memory $CD4^+$ T cells, is useful for diagnosing a deterioration in the immune function in animals with AIDS (26, 38, 48). Although this parameter usually correlates with the percentage of $CD4^+$ T cells, remarkable differences were noted between two Env vaccine groups after the challenge infection. First, all animals in the wt-Env vaccine group showed an increased percentage of this subset in the chronic phase (Fig. 6B). Second, three of the Δ5G Env vaccinees had a marked decrease after the challenge infection (Mm0001, Mm0002 and Mm0009), whereas the remaining animal (Mm0003) showed an increased percentage of this subset. In

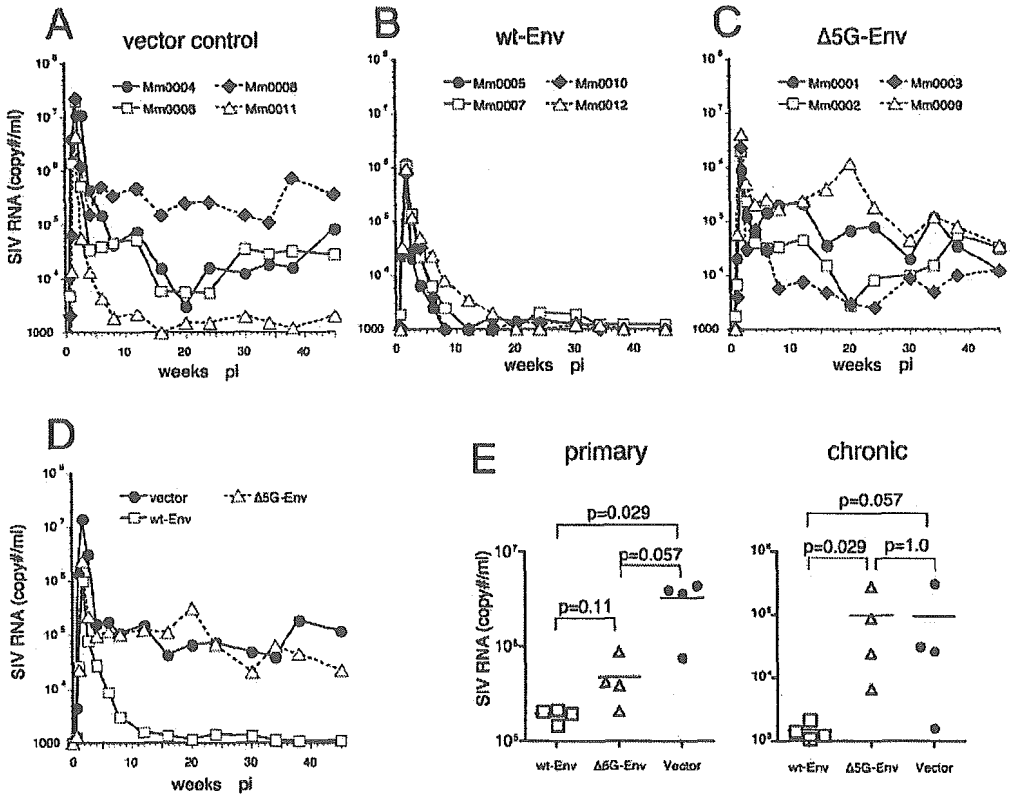


FIG. 5. Plasma viral loads after SIVmac239 challenge infection. Plasma viral load was measured by real-time PCR with a detection limit of 1,000 copies/ml. A: wt-Env vaccine group; B: Δ5G Env vaccine group; C: vector controls; D: comparison of viral loads among three groups; E: comparison of viral loads during the primary infection (5 days to 6 weeks p.i.) and chronic infection (8 weeks to 45 weeks p.i.) among three groups. Viral load was determined by averaging over a period of time.

vector controls, this subset remained in the range before the challenge infection in all animals but one (Fig. 6B).

**Env-specific-T-cell immunity after the challenge infection.** The magnitude of Env-specific T cells after the challenge infection is assumed to be influenced not only by vaccination but also by viral replication. Namely, SU-specific T cells at 4 days p.i. and those at 12 days p.i. were likely influenced by the former and the latter respectively. The magnitudes of SU-specific $CD4^+$ T cells and $CD8^+$ T cells at 4 days p.i. were comparable to those before challenge at 26 weeks p.p. (Fig. 3A and B); therefore, twofold-more SU-specific $CD8^+$ T cells and $CD4^+$ T cells were present in wt-Env vaccinees than in Δ5G Env vaccinees up to 4 days p.i. (Fig. 3C). However, this difference in the magnitudes of SU-specific $CD8^+$ T and $CD4^+$ T cells was not sustained at 7 and 12 days p.i. (Fig. 3C). Present with robust viral replication in primary infection, SU-specific $CD4^+$ T cells immediately decreased to an undetectable level at 12 days p.i. In contrast, SU-specific $CD8^+$ T cells increased (Fig. 3A and B). Subsequently, SU-specific $CD8^+$ T cells gradually decreased to very low or undetectable levels by 34 weeks p.i. (Fig. 3A). Thus, vaccine-induced SU-specific $CD8^+$ T and $CD4^+$ T cells were sustained only for a short period of time after challenge infection in both Env vaccine groups.

**SIV-specific T-cell immunity after challenge infection.** Despite an Env vaccination, robust SIV infection occurred shortly after the challenge infection (Fig. 5B and C). Consequently, SIV-specific $CD8^+$ T cells and $CD4^+$ T cells were elicited not only in vector controls but also in Env vaccine groups (Fig. 7A and B). To examine the effect of these SIV-specific T cells on the control of SIV infection, all animals were divided into SIV infection-controlled (controlled) and SIV infection-uncontrolled (uncontrolled) animals. Viral loads in chronic infection and the percentage of $CD4^+$ cells in PBMCs were used to classify the animals as controlled or uncontrolled (Fig. 6A). All animals in the wt-Env vaccine group, Mm00011 in vector controls, and Mm0003 in the Δ5G Env vaccine group were grouped as control animals. The remaining animals, Mm0004, Mm0006, and Mm0008 in vector controls and Mm0001, Mm0002, and Mm0009 in the Δ5G Env vaccine group were grouped as uncontrolled animals. Notably, SIV-specific $CD4^+$ T cells as well as the percentage of $CD4^+$ CD29H cells remained high in the chronic phase in controlled animals (Fig. 7B and 6B, respectively).

Although overall SIV-specific $CD8^+$ T cells were high in Env-vaccinated controlled animals, such correlation was not seen in vector controls grouped as uncontrolled animals (Fig. 7A). Therefore, to examine the relevance of virus-specific T cells to the control of SIV infection, the magnitudes of every viral-protein-specific T cell in controlled and uncontrolled animals were compared. As shown in Fig. 7C, Gag-specific $CD8^+$ T cells and $CD4^+$ T cells, and Tat/Rev-specific $CD4^+$ T cells

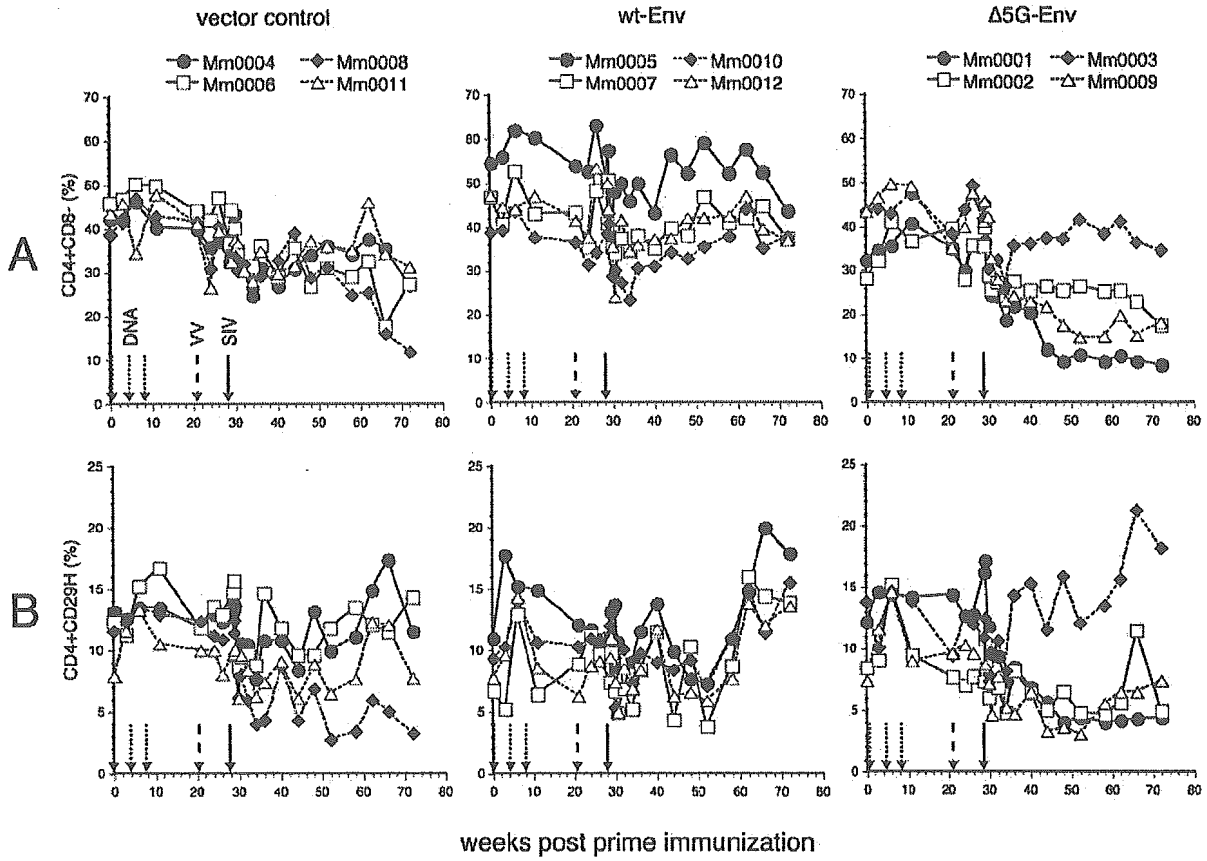


FIG. 6. $CD4^+$ T cells in PBMCs from rhesus macaques during immunization and after the challenge infection. A: Percentage of $CD4^+$ T cells in PBMCs; B: percentage of $CD4^+$ CD29high T cells in PBMCs.

were induced, with statistical significance ($P < 0.05$), in the control animals.

## DISCUSSION

The heavily glycosylated structure of Env has been considered a main cause of chronically persistent viral replication and the pathogenicity of HIV/SIV, primarily because it potentially interferes with the development of the host immune response associated with protective immune functions, such as NAb and CTL (10, 36, 44). This characteristic constitutes the primary reason for the difficulty of developing effective vaccines. We therefore examined the efficacy of a deglycosylated-Env vaccine and compared it with the wt-Env vaccine. This study showed that quintuple deglycosylation neither improved the immunogenicity of the wt-Env vaccine nor elicited NAb against SIVmac239. This was in contrast to what occurred with Δ5G infection in rhesus macaques, because the host response elicited by Δ5G infection not only contained Δ5G infection but also protected the animals from SIVmac239 challenge infection (36). This study therefore suggested that an almost sterilizing immunity against SIVmac239 induced in Δ5G-infected animals could not be explained by the immunogenicity of Δ5G Env; instead, it is likely associated with the property of Δ5G as an attenuated virus. In fact, Δ5G was more neutralization-sensitive than SIVmac239 (36). Alternatively, the immunogenic property of Env in Δ5G could not successfully be duplicated by immunization with a Δ5G Env DNA prime-vaccinia virus boost regimen. Therefore, another immunization regimen might be able to elicit the protective immune response induced by Δ5G infection.

The Env vaccine is superior to other vaccines containing other viral proteins with respect to the induction of NAb; however, both the Δ5G Env vaccine and the wt-Env vaccine could not induce detectable NAb against either SIVmac239 or Δ5G. Instead, the wt-Env vaccine induced higher NAb against macrophage-tropic SIV than the Δ5G Env vaccine. Notably, this parameter most significantly correlated with the efficacies of the two Env vaccines. As Ab neutralized the macrophage-tropic variant 239/envMERT, which has only four separate amino acid substitutions distributed in *env* of SVmac239 (34), it might recognize unknown epitopes conserved between SIVmac239 and 239/envMERT. On the other hand, Δ5G Env may not sufficiently present this epitope due to mutations. Regarding the role of nonneutralizing Ab for the control of SIVmac239 infection, it is assumed that, as the neutralization assay did not necessarily reflect in vivo conditions, such nonneutralizing Ab with potential virus-binding ability may interfere with SIVmac239 infection in animals. Alternatively, Ab

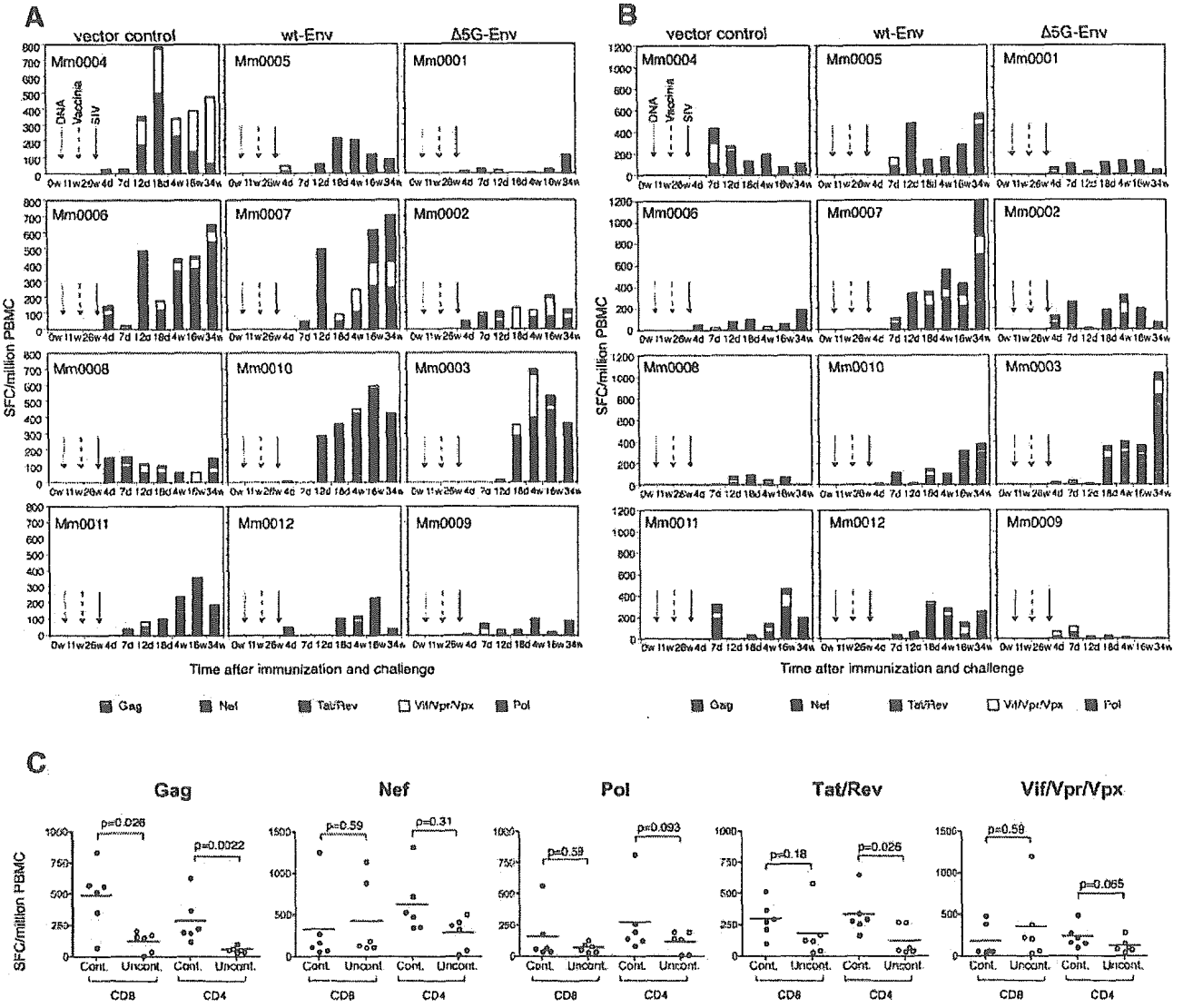


FIG. 7. SIV-specific $CD8^+$ T-cell and $CD4^+$ T-cell responses in 12 animals. A: SIV viral-protein-specific $CD8^+$ T cells in PBMCs were measured by ELISPOT assay for IFN-γ in three groups: vector controls, wt-Env vaccine group, and Δ5G Env vaccines. B: SIV viral-protein-specific $CD4^+$ T cells in PBMCs were measured by ELISPOT assay for IFN-γ in three groups. ELISPOT results of individual SIV proteins are colored as follows: Gag (red), Nef (green), Tat/Rev (blue), Vif/Vpr/Vpx (yellow), and Pol (pink). C: Comparison of cumulated $CD8^+$ T cells or $CD4^+$ T cells specific to the viral proteins Gag, Pol, Nef, Tat/Rev, and Vif/Vpr/VpX between SIV infection-controlled and uncontrolled animals. w, weeks; d, days.

might play a role in other effector functions, such as antibody-dependent cell-mediated cytotoxicity to eliminate the infected cells. The antibody-mediated enhancement of viral antigen processing and cross presentation is also a mechanism potentially related to the control of SIV infection in vivo (49).

Reduced immunogenicity in the Δ5G Env vaccine was also noted in cellular immunity. The levels of stimulation of antigen-specific $CD8^+$ T cells and $CD4^+$ T cells are MHC I and MHC II dependent, respectively. As the macaques in this study have different MHC haplotypes (data not shown), the magnitude and breadth of SIV-specific T cells should vary among the animals. Nevertheless, the magnitude of SU-specific $CD8^+$ T cells and $CD4^+$ T cells in PBMCs was greater in the wt-Env vaccine group than in the Δ5G Env vaccine group. Although the expression of SU by expressing plasmids and that of Env by the vaccinia virus vector elicited by either the wt-Env vaccine or Δ5G Env vaccine were indistinguishable in cultured cells (Fig. 2), wt-Env might persist longer than Δ5G Env in vaccinated animals. T-cell epitopes in the wt-Env vaccine might therefore be more efficiently presented on MHC molecules in antigen-presenting cells than in the Δ5G Env vaccine. Differences in glycosylation levels might also affect some processes in antigen-presenting cells associated with the presentation of T-cell epitopes in Env.

Taking all results together, Env glycosylation might affect the presentation of B-cell epitopes and T-cell epitopes required for Ab-mediated and T-cell-mediated immunities related to the control of SIV infection.

As seen in viral loads and SU-specific T cell levels after challenge infection (Fig. 3 and 5), the effect of vaccination was limited. That seemed related to the development of escape mutants. Therefore, distinctive cellular immune responses after the challenge infection were also implicated in the control of SIVmac239 replication. The magnitude of virus-specific $CD8^+$ T cells did not always correlate with the suppression of viral replication as reported previously (1, 6), particularly in vector controls (Fig. 5 and 7A); however, selected epitope-specific CTL responses might be associated with infection control. Gag-specific CTLs are such candidates, because a high magnitude of Gag-specific $CD8^+$ T cells was significantly elicited in five control animals (Fig. 7C). The magnitude of Gag- or Tat/Rev-specific $CD4^+$ T cells was statistically correlated with infection control (Fig. 7C). This may simply indicate a lower depletion of virus-specific $CD4^+$ T cells in animals with lower viral loads as reported previously (11). Alternatively, these virus-specific $CD4^+$ T cells may play an important role in protective immunity (39). Taken together, these results implicated the dominant role of selected epitope-specific $CD4^+$ T cells and $CD8^+$ T cells for the control of SIVmac239 infection.

The challenge virus that should be used has been an important issue in AIDS vaccine studies (8, 10, 12). Many studies have reported impressive efficacy in a pathogenic-SHIV macaque model (3, 4, 45, 46); however, pathogenic SHIVs use CXCR4 as a coreceptor, whereas the majority of clinical isolates of HIV-1 use CCR5 (13, 27). Therefore, the challenge virus for an AIDS vaccine study should be an R5 virus, such as SIV (10). Consistent with this concern, a DNA prime–modified-vaccinia virus Ankara boost regimen, inducing broad SIV-specific T-cell responses, reduced the initial viral replication but did not prevent disease progression against SIVmac239 challenge (18). Thus, vaccine studies using pathogenic SHIV should be reevaluated by using an R5 virus (10).

Matano et al. reported that a DNA prime-Sendai virus boost regimen induced the CTL-based control of SIVmac239 in rhesus macaques (27). This study demonstrated that a DNA prime-vaccinia virus WR boost regimen expressing only Env controlled the chronic infection of SIVmac239 in rhesus macaques. The relatively lower viral loads in macaques from Myanmar or Laos than in those of Indian origin might contribute to the control of SIVmac239 infection. Nevertheless, it is important that these two studies demonstrated the efficacies of the two vaccine regimens against highly pathogenic SIVmac239. In earlier studies, other R5 SIVs were used as a challenge virus for an efficacy study of vaccine candidates. An Env-based vaccine in vaccinia virus vector priming and subunit protein boosting protected cynomologous macaques against homologous SIVmne clone E11S (42). In recombinant modified vaccinia virus, Ankara viruses expressing Gag-Pol and/or Env exhibited vaccine efficacy because of reduced viremia and the increased survival of rhesus macaques infected with uncloned SIVsmE660 (41). Accordingly, the efficacy of vaccine candidates might be influenced by the experimental conditions. Thus, well-defined animal models with detailed virological, immunological, and genetic information and suitable challenge viruses are required for the evaluation of vaccine candidates and the development of an AIDS vaccine.

This study demonstrated the importance of Env as a component of the AIDS vaccine, and Env-specific $CD8^+$ and $CD4^+$ T cells and nonneutralizing Env-specific Ab were suggested as protective immunity components. Quintuple deglycosylation in Env reduced vaccine efficacy and Env-specific immune responses. Env may therefore be comprised of appropriate antigenic properties to elicit humoral and cellular immune responses required for protective immunity against homologous or allele-specific target SIV/HIV. These properties could be modified by the alteration of glycosylation.

In conclusion, although Env is an important immunogen for the AIDS vaccine, Env properties, including glycosylation, should be carefully considered to design vaccines specific to the targeted viruses.

## ACKNOWLEDGMENTS

We thank Kayoko Ueda for excellent technical assistance.

This work was supported by AIDS research grants from the Health Sciences Research Grants, from the Ministry of Health, Labor, and Welfare in Japan, and from the Ministry of Education, Culture, Sports, Science and Technology in Japan.

## REFERENCES

1. **Addo, M. M., X. G. Yu, A. Rathod, D. Cohen, R. L. Eldridge, D. Strick, M. N. Johnston, C. Corcoran, A. G. Wurcel, C. A. Fitzpatrick, M. E. Feeney, W. R. Rodriguez, N. Basgoz, R. Draenert, D. R. Stone, C. Brander, P. J. Goulder, E. S. Rosenberg, M. Altfeld, and B. D. Walker.** 2003. Comprehensive epitope analysis of human immunodeficiency virus type 1 (HIV-1)-specific T-cell responses directed against the entire expressed HIV-1 genome demonstrate broadly directed responses, but no correlation to viral load. J. Virol. **77**:2081–2092.
2. **Allen, T. M., and D. I. Watkins.** 2001. New insights into evaluating effective T-cell responses to HIV. AIDS **15**(Suppl. 5):S117–S126.
3. **Amara, R. R., F. Villinger, J. D. Altman, S. L. Lydy, S. P. O'Neil, S. I. Staprans, D. C. Montefiori, Y. Xu, J. G. Herndon, L. S. Wyatt, M. A. Candido, N. L. Kozyr, P. L. Earl, J. M. Smith, H. L. Ma, B. D. Grimm, M. L. Hulsey, J. Miller, H. M. McClure, J. M. McNicholl, B. Moss, and H. L. Robinson.** 2001. Control of a mucosal challenge and prevention of AIDS by a multiprotein DNA/MVA vaccine. Science **292**:69–74.
4. **Barouch, D. H., S. Santra, J. E. Schmitz, M. J. Kuroda, T. M. Fu, W. Wagner, M. Bilska, A. Craiu, X. X. Zheng, G. R. Krivulka, K. Beaudry, M. A. Lifton, C. E. Nickerson, W. L. Trigona, K. Punt, D. C. Freed, L. Guan, S. Dubey, D. Casimiro, A. Simon, M. E. Davies, M. Chastain, T. B. Strom, R. S. Gelman, D. C. Montefiori, M. G. Lewis, E. A. Emini, J. W. Shiver, and N. L. Letvin.** 2000. Control of viremia and prevention of clinical AIDS in rhesus monkeys by cytokine-augmented DNA vaccination. Science **290**:486–492.
5. **Berger, E. A., P. M. Murphy, and J. M. Farber.** 1999. Chemokine receptors as HIV-1 coreceptors: roles in viral entry, tropism, and disease. Annu. Rev. Immunol. **17**:657–700.
6. **Betts, M. R., D. R. Ambrozak, D. C. Douek, S. Bonhoeffer, J. M. Brenchley, J. P. Casazza, R. A. Koup, and L. J. Picker.** 2001. Analysis of total human immunodeficiency virus (HIV)-specific CD4(+) and CD8(+) T-cell responses: relationship to viral load in untreated HIV infection. J. Virol. **75**:11983–11991.
7. **Burton, D. R.** 2002. Antibodies, viruses and vaccines. Nat. Rev. Immunol. **2**:706–713.
8. **Burton, D. R., R. C. Desrosiers, R. W. Doms, W. C. Koff, P. D. Kwong, J. P. Moore, G. J. Nabel, J. Sodroski, I. A. Wilson, and R. T. Wyatt.** 2004. HIV vaccine design and the neutralizing antibody problem. Nat. Immunol. **5**:233–236.
9. **Chapman, B. S., R. M. Thayer, K. A. Vincent, and N. L. Haigwood.** 1991. Effect of intron A from human cytomegalovirus (Towne) immediate-early gene on heterologous expression in mammalian cells. Nucleic Acids Res. **19**:3979–3986.
10. **Desrosiers, R. C.** 2004. Prospects for an AIDS vaccine. Nat. Med. **10**:221–223.
11. **Douek, D. C., J. M. Brenchley, M. R. Betts, D. R. Ambrozak, B. J. Hill, Y. Okamoto, J. P. Casazza, J. Kuruppu, K. Kunstman, S. Wolinsky, Z. Grossman, M. Dybul, A. Oxenius, D. A. Price, M. Connors, and R. A. Koup.** 2002. HIV preferentially infects HIV-specific CD4+ T cells. Nature **417**:95–98.
12. **Emini, E. A., and W. C. Koff.** 2004. AIDS/HIV. Developing an AIDS vaccine: need, uncertainty, hope. Science **304**:1913–1914.
13. **Feinberg, M. B., and J. P. Moore.** 2002. AIDS vaccine models: challenging challenge viruses. Nat Med. **8**:207–210.
14. **Gardner, M. B.** 2003. Simian AIDS: an historical perspective. J. Med. Primatol. **32**:180–186.
15. **Gotoh, H., T. Shioda, Y. Sakai, K. Mizumoto, and H. Shibuta.** 1989. Rescue